Cell Reports
Medicine

Article

CD28-CAR-T cell activation through FYN kinase signaling rather than LCK enhances therapeutic performance

Graphical abstract

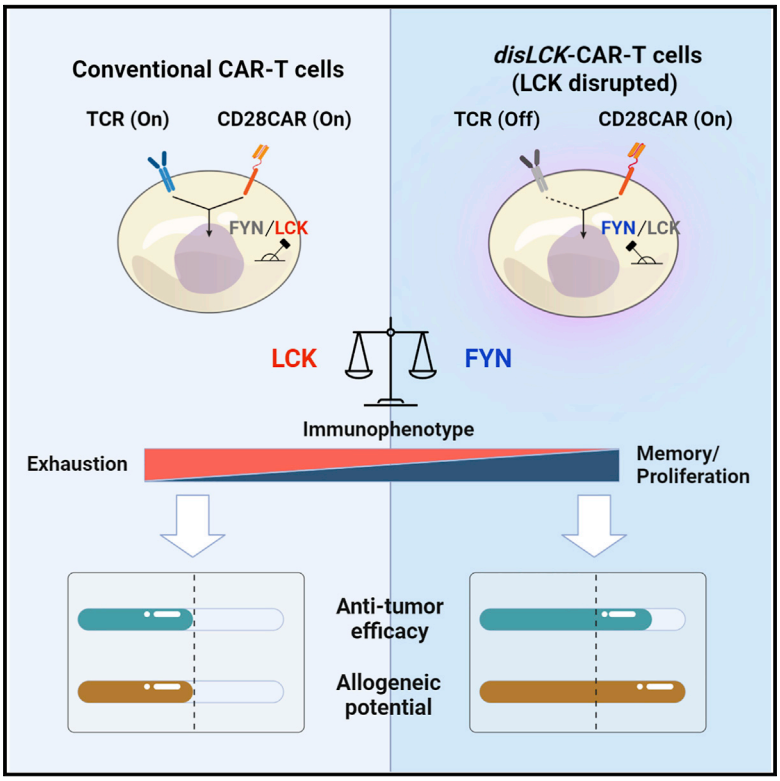

Highlights

- Chimeric antigen receptors (CARs) can initiate signaling in T cells lacking LCK
- CD28 domain and SRC family kinase FYN play a role in LCK-independent CAR signaling
- Disrupting LCK in CAR-T cell (*disLCK*-CAR-T) improves the function and immunophenotype
- *DisLCK*-CAR-T shows elevated anti-tumor efficacy and the potential for allogeneic use

Authors

Ling Wu, Joanna Brzostek, Previtha Dawn Sakthi Vale, ..., Junyun Lai, Paul A. MacAry, Nicholas R.J. Gascoigne

Correspondence

micnrjg@nus.edu.sg

In brief

Wu et al. discover that LCK, an essential kinase for TCR signaling, is dispensable for CAR signaling. CD28 domain and the kinase FYN mediate this LCK-independent signaling. LCK-disrupted CAR-T shows increased *in vivo* anti-tumor efficacy—attributed to the improved memory/persistence and reduced exhaustion—and the potential for allogeneic use.

Wu et al., 2023, Cell Reports Medicine *4*, 100917
February 21, 2023
https://doi.org/10.1016/j.xcrm.2023.100917

CellPress

Cell Reports Medicine

CellPress
OPEN ACCESS

Article

CD28-CAR-T cell activation through FYN kinase signaling rather than LCK enhances therapeutic performance

Ling Wu,[1,2] Joanna Brzostek,[1,2] Previtha Dawn Sakthi Vale,[1,2] Qianru Wei,[2] Clara K.T. Koh,[1,2] June Xu Hui Ong,[1,2] Liang-zhe Wu,[1,2] Jia Chi Tan,[1,2] Yen Leong Chua,[1,2] Jiawei Yap,[1,2] Yuan Song,[1,2,3] Vivian Jia Yi Tan,[1,2] Triscilla Y.Y. Tan,[2] Junyun Lai,[2,3] Paul A. MacAry,[1,2,3,4] and Nicholas R.J. Gascoigne[1,2,4,5,*]

[1]Immunology Translational Research Programme, Yong Loo Lin School of Medicine, National University of Singapore, 5 Science Drive 2, Singapore 117545, Singapore

[2]Department of Microbiology and Immunology, Yong Loo Lin School of Medicine, National University of Singapore, 5 Science Drive 2, Singapore 117545, Singapore

[3]Immunology Programme, Life Sciences Institute, National University of Singapore, Singapore, Singapore

[4]Cancer Translational Research Programme, Yong Loo Lin School of Medicine, National University of Singapore, Singapore, Singapore

[5]Lead contact

*Correspondence: micnrjg@nus.edu.sg

https://doi.org/10.1016/j.xcrm.2023.100917

SUMMARY

Signal transduction induced by chimeric antigen receptors (CARs) is generally believed to rely on the activity of the SRC family kinase (SFK) LCK, as is the case with T cell receptor (TCR) signaling. Here, we show that CAR signaling occurs in the absence of LCK. This LCK-independent signaling requires the related SFK FYN and a CD28 intracellular domain within the CAR. LCK-deficient CAR-T cells are strongly signaled through CAR and have better *in vivo* efficacy with reduced exhaustion phenotype and enhanced induction of memory and proliferation. These distinctions can be attributed to the fact that FYN signaling tends to promote proliferation and survival, whereas LCK signaling promotes strong signaling that tends to lead to exhaustion. This non-canonical signaling of CAR-T cells provides insight into the initiation of both TCR and CAR signaling and has important clinical implications for improvement of CAR function.

INTRODUCTION

Adoptive T cell therapy using chimeric antigen receptor T cells (CAR-T cells) shows great clinical success.[1,2] The cytoplasmic domains of CD28 or CD137 (4-1BB) are widely used in CAR design.[3] Nevertheless, the molecular mechanism of CAR signal transduction and how the co-stimulatory domain interplays with CD3ζ immunoreceptor tyrosine-based activation motif (ITAM) signals are poorly understood. In part, this is due to the assumption that CAR and T cell receptor (TCR) signaling are very similar because of the sharing of signaling domains. Phosphoproteome analysis of signaling by TCR, CD28-CD3ζ, and CD137-CD3ζ CARs did not find divergent signaling pathways.[4] Rather, the differences were in signaling strength and kinetics.[4–7]

However, CAR signal transduction is potentially significantly different from what we understand of TCR signaling. Second- and later-generation CARs contain integral co-stimulatory elements, ensuring that co-stimulation occurs at the same time and places as antigen recognition, which is not the case for normal T cell activation. The formation of the CAR-T immunological synapse (IS) is different and less structured than that of normal T cells.[3,5] The CD28 domain increases the phosphorylation rate of CD3ζ,[8] whereas CD137 was found to recruit the THEMIS-SHP1 complex to the signalosome, resulting in decreased CAR signaling.[9] It is therefore critical to understand how CAR transduces signaling such that therapeutic performance can be optimized.

In this work, we show that CARs with a CD28 domain, unlike TCRs, effectively transduce signaling in the absence of LCK, without which TCR signaling is totally abrogated and thymocyte development is profoundly blocked in *Lck* knockout mice.[10,11] Here, we find that another SRC family kinase (SFK), FYN, can phosphorylate the CAR ITAMs. We demonstrate that LCK-disrupted CAR-T cells (*disLCK*-CAR-T) have special characteristics *in vitro* and *in vivo*. They only transduce signals through the CAR, not through endogenous TCRs. Therefore, *disLCK*-CAR-T cells could provide an alternative approach to generate allogeneic CAR-T cells without knocking out TCRs. We show that *disLCK*-CAR-T cells become more memory-like *in vivo*, with a less exhausted phenotype than conventional CAR-T cells, resulting in increased persistence and significantly improved efficacy. Signal network analysis indicates that the altered characteristics of *disLCK*-CAR-T cells could be caused by the increase of FYN-associated proliferation and survival pathways and by the decrease of strongly activated immune responses via LCK. In summary, this non-canonical LCK-independent CAR signaling

sheds light on how CAR signaling is transduced and shows that we can use special aspects of CAR-T signal transduction to improve CAR-T technology.

RESULTS

CAR-T cells can transduce T cell signaling without LCK

In our previous study, we compared signaling from a TCR with that from a second-generation CD28-CAR where both the target LMP2A peptide (L2)-major histocompatibility complex (MHC) complex (Figure S1A).[12,13] We used CHO cells expressing single-chain peptide MHC (pMHC) as antigen-presenting cells (APCs) (Figures S1B and S1C).[14] We found that anti-pMHC CARs have similar biophysical properties to TCR[15] but that the CD8 co-receptor is dispensable for CAR signaling.[14] CD8 is typically considered to be important for bringing LCK into the IS.[16,17] Since CD8 was not able to enhance CAR-T signaling, we hypothesized that LCK might not be critical for CAR signaling, at least with regard to CD8-bound LCK. Surprisingly, unlike TCR, CAR was able to activate signaling in the absence of LCK, where CAR-Jcam cells produced interleukin-2 (IL-2) normally and showed phosphorylation of signaling molecules similar to TCR-Jurkat cells where LCK is present (Figures 1A, 1B, and S1D). We used CRISPR-Cas9 to perform homologous direct repair (HDR) to insert an anti-CD19 CD28-CAR construct, with either an Myc or His tag, into the *LCK* locus to disrupt its expression in primary $CD8^+$ T cells (Figure 1C). Distinct populations of CAR^+ $CD8^+$ T cells were detected after HDR: CAR-Myc^+, CAR-His^+, and a double-positive population. Genotyping the insertion site of the total CAR^+ population confirmed that the *CAR* construct was inserted into the *LCK* locus (Figure S1E). After sorting of each single and double CAR^+ population, LCK expression was dramatically reduced in *LCK*-CAR-His and completely depleted in *LCK*-CAR-DP cells (Figures S1F and 1E). The *LCK*-CAR-DP cells seemed to have no significant difference in cytotoxicity compared with *LCK*-CAR-His and *LCK*-CAR-Myc cells. However, there was stronger cytokine secretion by *LCK*-CAR-DP cells (Figures 1F and 1G). These data imply that CAR signaling has an altered signal-triggering mechanism and that LCK, essential for TCR signaling, is dispensable for CAR signaling.

LCK-independent CAR signaling relies on CD28 co-stimulatory domain

CAR differs from TCR in many ways, particularly in its chimeric design. To identify which domains in CAR enable LCK-independent signaling, we replaced domains in our CD28-CAR. For production simplicity, we collected total CAR^+, including both single and double knockin populations, as *disLCK*-CAR-T cells. They showed a significant reduction of LCK expression (Figure S2A). LCK-independent CAR signaling was not determined by antigen specificity since anti-HER2, like anti-CD19 CAR, initiated strong signaling in *disLCK*-CAR-T cells (Figure 2A). The CD3ζ domain and the co-stimulatory domain were required to initiate CAR signaling in the absence of LCK (Figures S2B and S2C). The CD28 co-stimulatory domain was crucial to support LCK-independent CAR signaling, but the CD137 co-stimulatory domain did not support it (Figures 2B and S2D). In a third-generation CAR containing both CD28 and CD137 domains, *disLCK*-CAR-T cell activation in response to antigen was observed but was much weaker compared with CD28-CAR. The PI3K-binding motif and proline-rich region are critical in CD28 signal transduction.[18] We tested CD28 domain deletion, mutation of PI3K-binding motif YMNM to FMNM, and alanine substitution of the prolines in the proline-rich region PYAP (where SFK binds) to AYAA.[19] LCK-independent CAR signaling was strongly reduced without the CD28 intracellular domain and by AYAA mutation (Figures 2C and S2E). To further substantiate the importance of CD28 to LCK-independent signaling, we expressed CD80 and CD86 in CHO-APCs to enable endogenous CD28 signaling activation in *trans* (Figure S2F). When endogenous CD28 was co-activated by CD80/86, tumor necrosis factor (TNF) and interferon γ (IFNγ) secretion of *disLCK*-CD137-CAR-T cells was restored (Figure 2D). LCK-deficient CAR1-Jcam and TCR-Jcam cells also showed restored IL-2 production and downstream signaling when CD28 co-stimulation was provided (Figures S2G–S2I). Thus, LCK-independent CAR signaling required a CD28 co-stimulatory signal, mediated at least partly through the PYAP motif, either from CD28 intracellular domain in CAR or from endogenous CD28 molecules.

SFK FYN mediates LCK-independent CAR signaling

To determine if any other SFK was responsible for initiation of LCK-independent CAR signaling, we used SFK pan-inhibitor PP2, resulting in inhibition of both CAR and TCR signaling in primary T cells as well as Jurkat cells (Figures 3A, S3A, and S3B). LCK and FYN are the main SFKs in T cells,[20] so we used the selective inhibitors A770041 and SU6656 to target LCK and FYN, respectively.[21,22] We initially used Jurkat T cells to study proximal TCR signaling,[23,24] finding that LCK-independent CAR signaling in primary T cells was also found as in Jurkat T cells, as shown above (Figures 1, 2, S1, and S2). TCR-Jurkat was ∼7-fold more sensitive to the LCK inhibitor, whereas CAR-Jurkat was ∼1.5-fold more sensitive to the FYN inhibitor (Figures S3C and S3D). These data suggested that FYN could be the kinase activating downstream signaling from CAR. Western blot analysis in LCK-deficient Jcam cells showed that the activation site Y420 of FYN, corresponding to SFK phosphorylation site Y416, was phosphorylated after CAR-Jcam, but not TCR-Jcam, engagement with specific APCs, with a nearly 2-fold increase in FYN pY420 after 30 min (Figure 3B). To better validate the role of LCK and FYN, we used CRISPR-Cas9 to knock out (KO) LCK or FYN in Jurkat. After gRNA screening (Table S1) and single-cell sorting (Figure S3E), LCK-KO clone 20 and FYN-KO clone 8 were selected for further experiments (Figure 3C). The expression of CAR or TCR was equivalent in FYN-KO Jurkat, and lack of FYN was confirmed in CAR- or TCR-Jurkat FYN-KO (Figures S3F and S3G). In LCK-KO Jurkat, CAR, but not TCR, was still functional, consistent with the results above. Conversely, IL-2 production by CAR-Jurkat FYN-KO was dramatically reduced compared with the wild type (Figure 3D). Immunoprecipitation experiments showed that CD28-CAR associated with FYN upon activation (Figure 3E). This association weakened after mutation of the CD28 domain, and the strength of FYN association corresponded with the activation level, suggested by IL-2 production, supported by mutated CD28-CAR (Figure 3F). These data showed that CAR signaling

CellPress
OPEN ACCESS

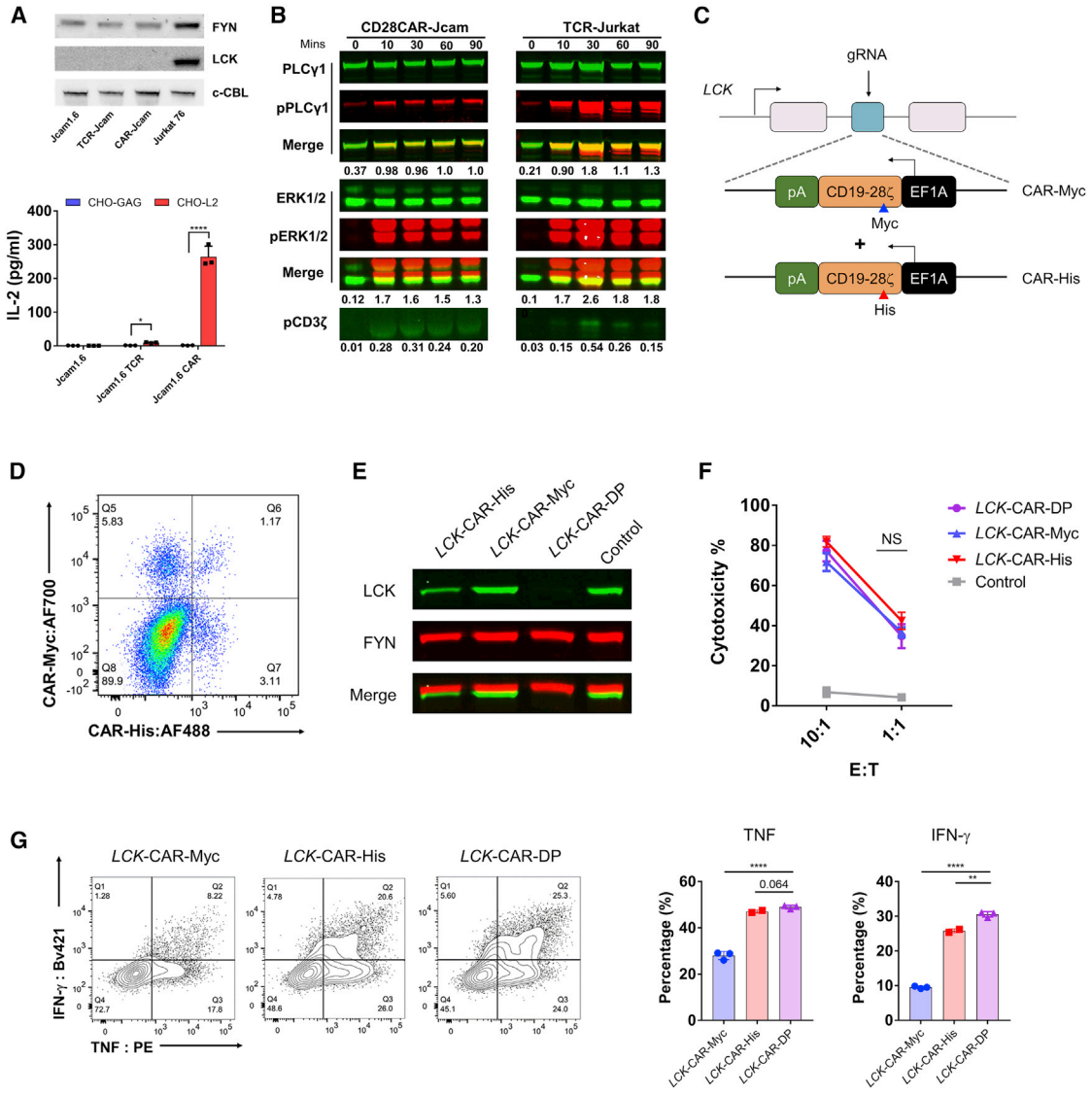

Figure 1. CAR-T cells can transduce T cell signaling without LCK

(A) Top: western blot detection of LCK or FYN expression in CAR or TCR-Jcam1.6 cell. Bottom: CAR or TCR responsiveness in LCK-deficient Jcam1.6 cells. CHO-L2 is the artificial APC presenting the $LMP2A_{426-434}$ (CLGGLLTMV) (L2) target peptide on HLA-A2. CHO-GAG presents the irrelevant GAG (SLYNTVATL) peptide.

(B) Phosphorylation of TCR signaling pathway molecules PLCγ1, ERK, and CD3ζ at different time points by LCK-deficient CD28CAR-Jcam cells. LCK-sufficient TCR-Jurkat cells were used as positive control. Phosphorylation of PLCγ1, ERK1/2, or CD3ζ was calculated relative to intensity of total PLCγ1, ERK, or ERK, respectively.

(C) Schematic of *LCK* locus-targeted homologous directed repair (HDR) by CRISPR-Cas9 editing. The anti-CD19-CD28CAR construct has either a Myc or His tag.

(D) CAR-His and CAR-Myc expression after *LCK* locus-targeted HDR.

(E) Western blot detection of LCK expression after sorting of CAR-His^+, CAR-Myc^+, and CAR-DP (Myc^+/His^+) $CD8^+$-T cells. Control represents mock-edited $CD8^+$-T cells.

(F) Cytotoxicity of CAR-His^+, CAR-Myc^+, and CAR-DP $CD8^+$-T cells. Control group was the target cells with mock-edited $CD8^+$-T cells.

(G) Cytokine secretion of CAR-His^+, CAR-Myc^+, and CAR-DP $CD8^+$-T cells upon activation. CAR-T cells were incubated with CD19-expressing Daudi cells at a 1:1 ratio for 18 h, then stained for intracellular TNF or IFNγ. The left panel is the representative fluorescence-activated cell sorting (FACS) data, and the right panel is the statistical summary and analysis.

All data are representative of 3 independent experiments, plotted as mean ± SD of technical triplicates. *$p < 0.05$; **$p < 0.01$; ***$p < 0.001$; ****$p < 0.0001$; not significant (NS) $p > 0.05$. (A)–(G) were analyzed by Student's t test.

See Figure S1 for additional data.

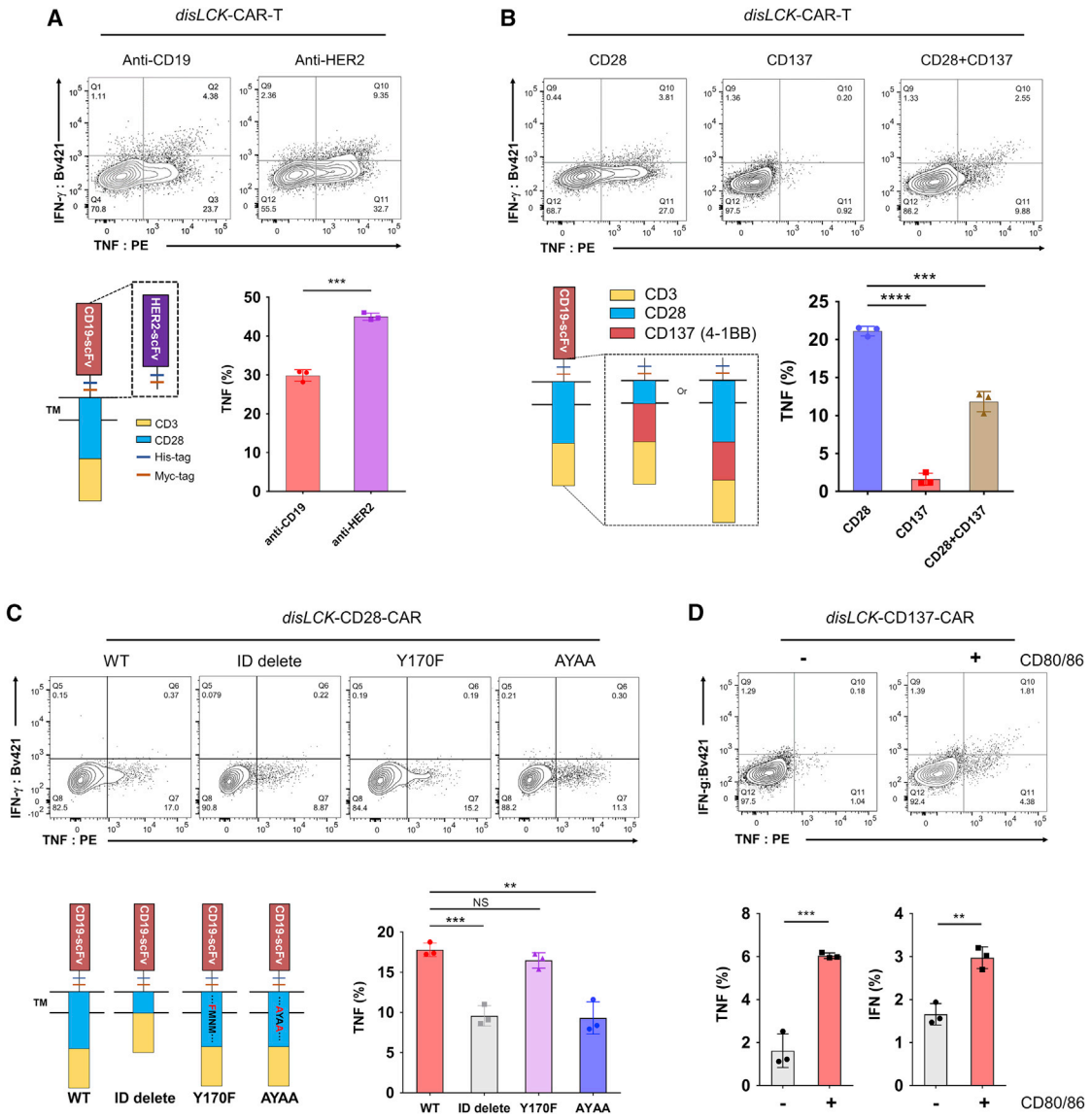

Figure 2. LCK-independent CAR signaling relies on CD28 co-stimulatory domain

(A) The effects of recognition domain in *disLCK*-CAR-T cell signaling. Anti-CD19-CD28CAR construct has been replaced with anti-HER2 scFv. CHO-CD19- and HER2-expressing SKBR3 cells were used as target cells and mixed with its respective *disLCK*-CAR-T cells at a 1:1 ratio for 18 h. The top panel is the representative FACS data, and the bottom panel is the schematic of the constructs with different recognition domains and an analytical summary.

(B) The effects of intracellular domain in *disLCK*-CAR-T cell signaling. The top panel is the representative FACS data, and the bottom panel is the schematic of the constructs with different intracellular domains and an analytical summary.

(C) Cytokine secretion of *disLCK*-CAR-T cells with different CD28-CAR mutations. The top panel is the representative FACS data, and the bottom panel is the schematic of CD28-CAR mutations and an analytical summary.

(D) Cytokine secretion of *disLCK*-CD137-CAR-T with or without CD80/CD86 co-stimulation on endogenous CD28. The top panel is the representative FACS data, and the bottom panel is the analytical summary.

Data are representative of 3 independent experiments, plotted as mean ± SD of technical triplicates. p values denoted as in the Figure 1 legend by Student's t test. See Figure S2 for additional data.

with CD28 domain was more sensitive to, and could rely on, FYN instead of LCK.

disLCK-CAR-T cells selectively activate CAR signaling

Given that CD28-CAR and TCR signaling are mediated by different SFKs, we hypothesized that *disLCK*-CAR-T cells would not be activated via TCR. To test this hypothesis, our L2 peptide-specific CAR and a TCR with specificity against E183-91 (FLLTRILTI) epitope from hepatitis B virus (HBV), hence referred to as E183-TCR,[25] were mono-transduced in Jurkat T cells designated as L2-CAR-T (1) and E183-TCR-T (2) or co-transduced into Jurkat (E183-TCR + L2-CAR-T [3]) or LCK-KO Jurkat

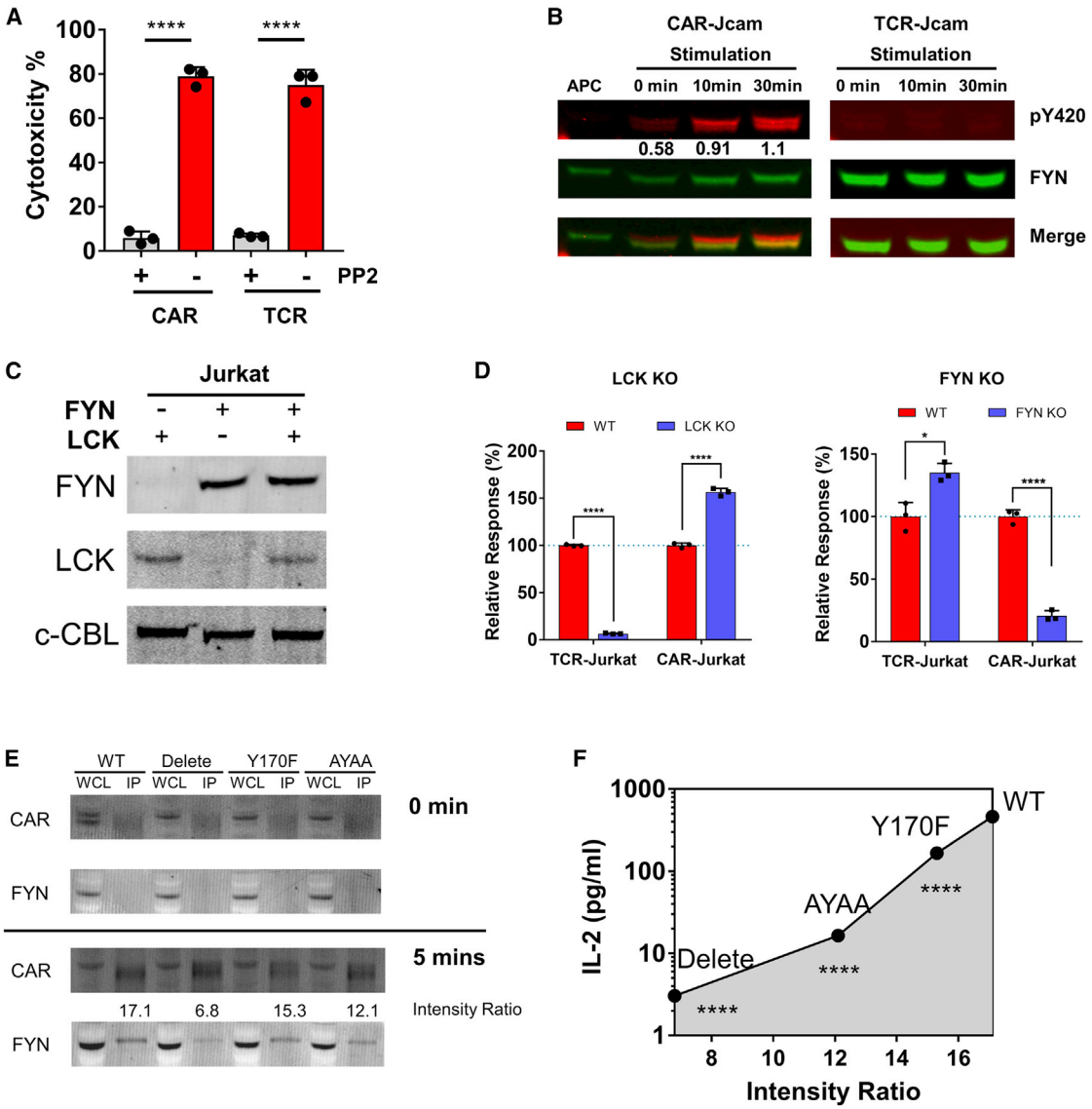

Figure 3. FYN is suggested to mediate CD28-CAR-T cell activation in the absence of LCK

(A) The cytotoxicity of primary CAR-T and TCR-T cells with or without PP2 inhibitor (10 μM). CAR-T targets CD19, and TCR-T targets HLA/A2-L2. Daudi cells, which express CD19 and were transduced with HLA/A2-L2, were used as target cells. The CAR-T cells were mixed with target cells at an E:T ratio of 4:1.

(B) Phosphorylation (pY420) of FYN in LCK-deficient CAR- or TCR-Jcam cells at different time points. APC stands for artificial antigen-presenting cell CHO-L2, to which the CAR and TCR responded. The number shown below indicates band intensity of pY420 relative to total FYN (FYN pY420 was stained by anti-pSRC family pY416).

(C) LCK and FYN expression in LCK or FYN-KO Jurkat clone after CRISPR-Cas9 editing. C-CBL was used as loading control.

(D) IL-2 production of TCR and CAR in LCK or FYN-KO Jurkat upon activation by CHO-L2.

(E) Association of FYN with CD28CAR variants. Jcam cells with different CD28CAR variants were activated by CHO-L2 for 5 min, and anti-Myc antibody was used to immunoprecipitate CAR. The association strength (intensity ratio) was calculated by the relative intensity of FYN to that of immunoprecipitated CAR.

(F) Correlation of FYN association strength with IL-2 production by Jcam cells with different CD28-CAR variants. The intensity ratio in abscissa is from (E), and the statistical significance is calculated by compare IL-2 production by CD28CAR variants with that of wild type (WT). The CAR and TCR mentioned above (B–E) both specifically target HLA/A2-L2, and CD28CAR was used.

Data are representative of 3 independent experiments (except 2 for E), plotted as mean ± SD of technical triplicates. p values denoted as in the Figure 1 legend by Student's t test.

See Figure S3 for additional data.

(E183-TCR + L2-CAR-LCK KO-T [4]) (Figures 4A and S4). The E183-TCR + L2-CAR-T (iii) cells were able to produce IL-2 upon stimulation by either CHO-E183 or CHO-L2, showing that activation of CAR and TCR was unimpaired in a dual CAR + TCR system. However, CHO-L2, but not CHO-E183, induced IL-2 production in the E183-TCR + L2-CAR-LCK KO-T (iv) cells

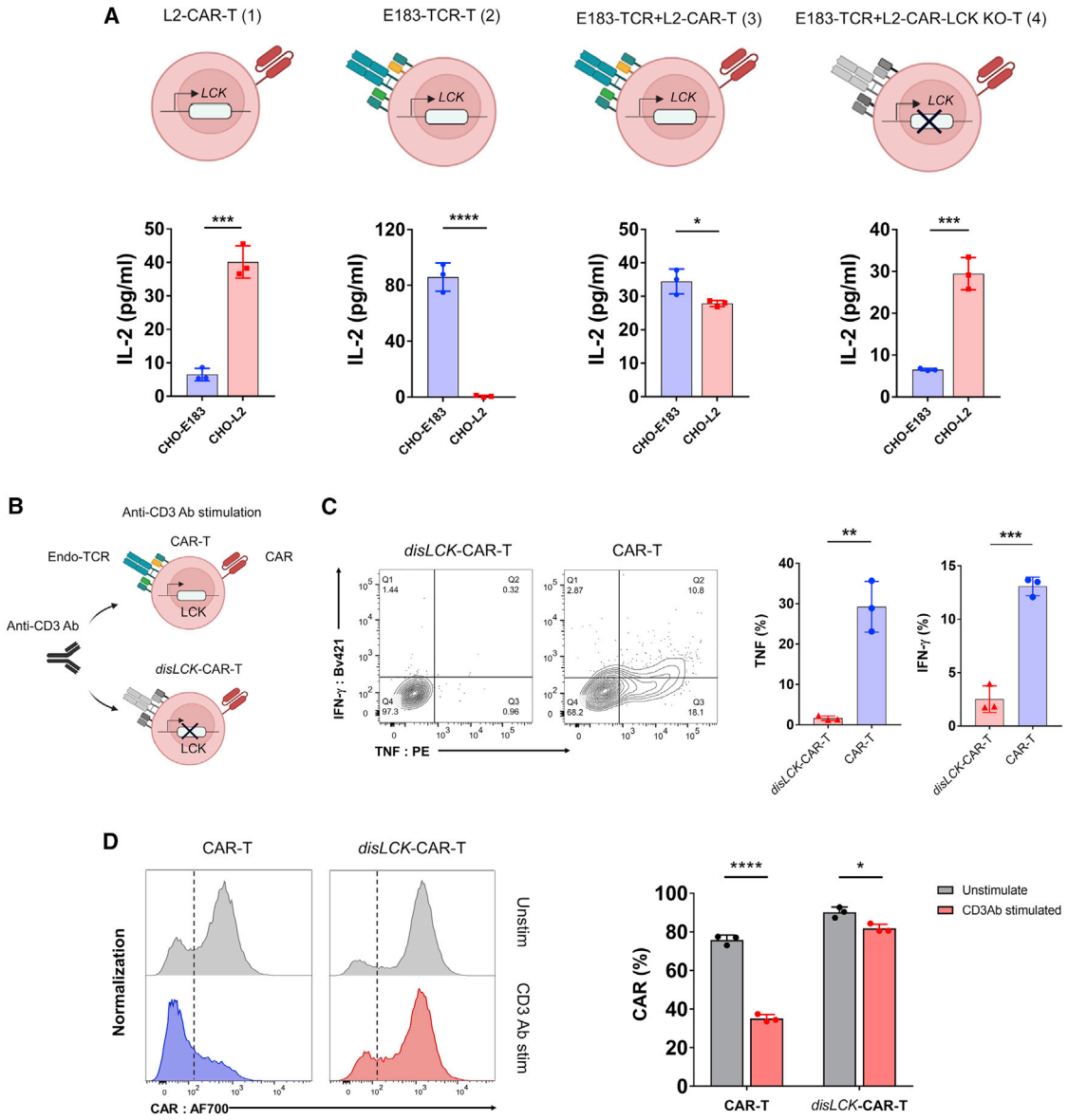

Figure 4. *disLCK*-CAR-T cells selectively activate CAR signaling

(A) TCR and CAR responsiveness selectivity in LCK-sufficient or -deficient Jurkat T cells. The top panel shows the schematics of E183 peptide-specific TCR (E183-TCR) or LMP2 peptide-specific CAR (L2-CAR) expressed in LCK-sufficient (1–3) or -deficient Jurkat T cells (4). The bottom panel shows the responsiveness of each group against CHO-E183 or CHO-L2, respectively. CHO-E183 is a mono-peptide CHO APC presenting only the E183 peptide. Similarly, CHO-L2 presents only the LMP2A peptide.

(B) Schematics of activation of endogenous TCR in *disLCK*-CAR-T or conventional CAR-T cells. Anti-CD3 Ab was used to activate endogenous TCR.

(C) Cytokine secretion of CAR-T cells upon anti-CD3 activation. The left panel is the representative data, and the right panel is the statistical summary and analysis.

(D) CAR expression after anti-CD3 antibody activation. The left panel is the representative data, and the right panel is the statistical summary and analysis.

Data are representative of 3 independent experiments, plotted as mean ± SD of technical triplicates. p values denoted as in the Figure 1 legend by Student's t test. See Figure S4 for additional data.

co-expressing CAR and TCR, showing that LCK deficiency allows signaling pathways for CAR, but not TCR, triggering (Figure 4A). In primary *disLCK*-CAR-T cells, anti-CD3 antibody (Ab) was used to activate endogenous TCR (Figure 4B). In contrast to CAR's ability to activate *disLCK*-CAR-T cells, TCR signaling was strongly reduced, whereas TCR signaling was functional in conventional CAR-T cells (Figure 4C). Interestingly, CAR expression in conventional CAR-T cells was strongly downregulated upon endogenous TCR activation by anti-CD3 Ab but not in *disLCK*-CAR-T cells (Figure 4D). These data suggest that TCR and CAR signal triggering are differentiated in *disLCK*-CAR-T cells.

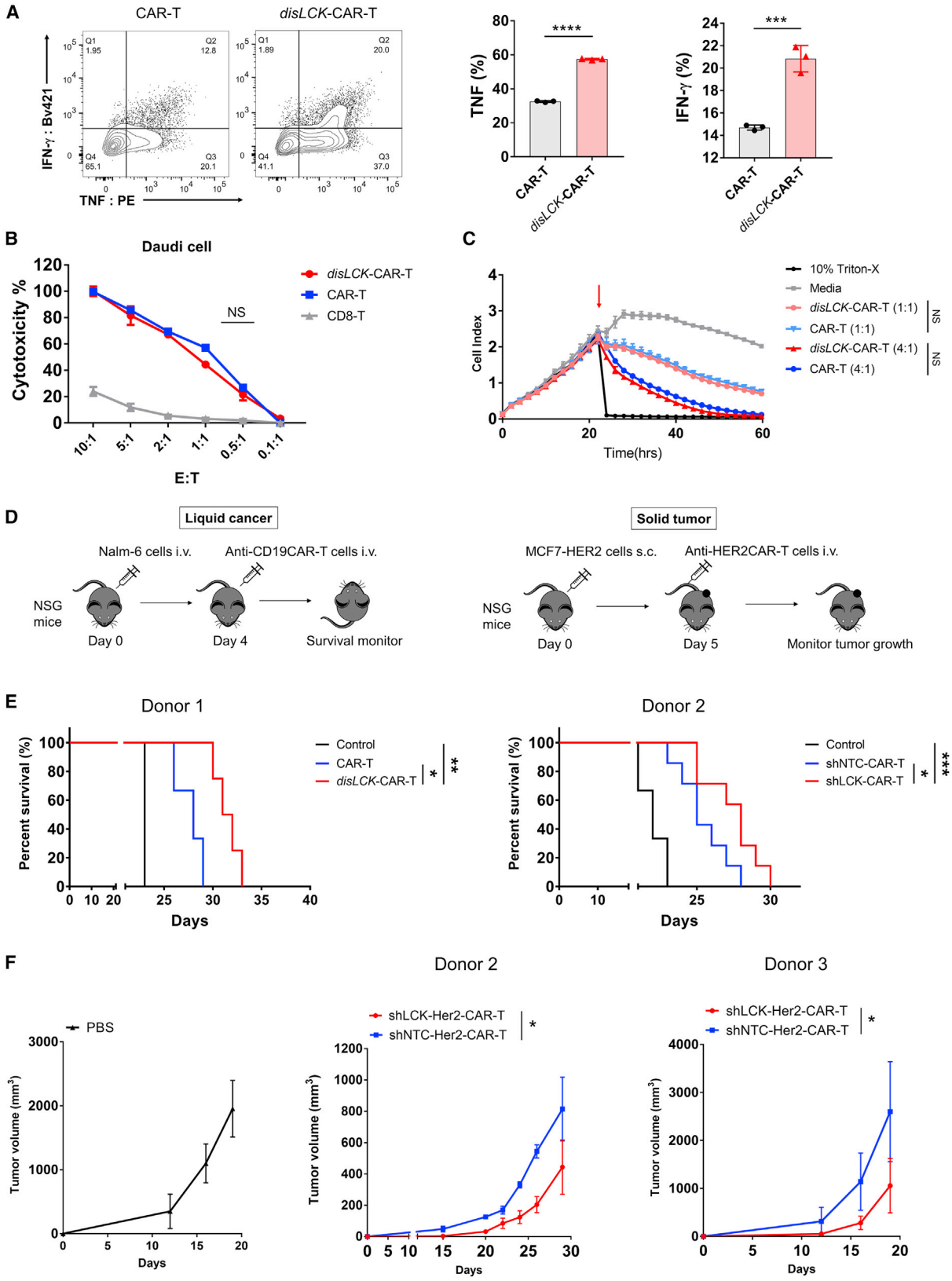

(legend on next page)

disLCK-CAR-T cells enhance *in vivo* therapeutic efficacy

To investigate functional consequences of LCK-independent CAR signaling and whether *disLCK*-CAR-T cells could have practical applications, we compared *disLCK*-CAR-T with conventional CAR-T cells *in vitro* and *vivo*. *disLCK*-CAR-T cells with comparable CAR expression to conventional CAR-T showed significantly higher activation for cytokine secretion (Figures 5A and S5A) but no significant difference in cytotoxicity (Figures 5B, 5C, and S5B–S5D). However, *in vivo* efficacy of CAR-T cells was enhanced after disruption of LCK expression, as evaluated in both liquid and solid tumor mouse models (Figure 5D). In a standard mouse leukemia model, where 5×10^5 CD19-expressing Nalm-6 cells were injected, *disLCK*-CAR-T significantly improved *in vivo* efficacy compared with conventional CAR-T cells (Figure 5E). To further validate the impact from LCK disruption, we implemented a short hairpin RNA (shRNA) method to knock down LCK expression in CAR-T cells, with a non-targeting shRNA as control. The shLCK-CAR-T cells had comparable CAR expression to non-targeting contro (shNTC)-CAR-T cells, but the LCK expression in shLCK-CAR-T cells was greatly reduced (Figures S5E and S5F). At the dose that CAR-T cells showed significant therapeutic efficacy versus control, the shLCK-CAR-T cells significantly improved the *in vivo* efficacy compared with shNTC-CAR-T cells in terms of mouse survival and Nalm-6 cell numbers *in vivo*, as detected by luciferase signal (Figures 5E, S5G, and S5H). In a solid tumor mouse model using a breast cancer cell line, MCF7 cells expressing HER2 (Figure 5D), shLCK-CAR-T cells showed significantly enhanced *in vivo* performance. Tumor growth in the shLCK-CAR-T cell-treated group was reduced more dramatically than the shNTC-CAR-T cell-treatment group (Figure 5F).

disLCK-CAR-T cell activation by FYN leads to a more proliferative, memory-retaining, and exhaustion-reduced state

FYN and LCK were reported to negatively regulate each other's activation.[20] This was observed when FYN and LCK were knocked out individually (Figure 3D). It is therefore possible that the activation profile of TCR signaling might be altered by more FYN activity when LCK is disrupted, leading to a distinct immunophenotype. This is predicted by analyzing which molecules in TCR signaling distinctly interact with FYN compared with LCK. We cross referenced and filtrated among different gene databases and curated a "TCR signaling molecules pool," which contains 1,440 molecules involved in TCR signaling. Among them, 330 molecules were identified to be linked with FYN or LCK. Their respective link scores to FYN and LCK were acquired via the String webtool. These molecules were further divided into FYN uniquely linked (58), FYN more-strongly linked (11), FYN and LCK shared linked (149), LCK more-strongly linked (10), and LCK uniquely linked (102) (Figure 6A). The more-strongly linked molecule is defined by difference between link score to FYN and to LCK >0.3, and the uniquely linked are the ones showing connections only either to FYN or to LCK. FYN uniquely and more-strongly linked molecules (69) or LCK uniquely and more-strongly linked molecules (112) were grouped and analyzed in the KEGG signal pathway database to show their distinct impacts on TCR signaling pathways. FYN-group molecules were more involved in proliferation and survival signaling pathways, including PI3K-AKT signaling, Rap1 signaling, MAPK signaling, and Ras signaling. LCK-group molecules were more involved in immune action pathways, such as Th1, Th2, and Th17 cell differentiation. These signal pathway involvements were further substantiated by clustering the molecular links within the FYN or LCK groups (Figures S6A and S6B). This result implies that *disLCK*-CAR-T cells could be more prone to proliferation and survival by enhanced FYN activity and would prevent exhaustion from overactivated immune responses.

In vitro evaluation of *disLCK*-CAR-T supported this implication. As shown in Figure 6B, the *disLCK*-CAR-T proliferated strongly upon antigen stimulation. Differences in the quiescent state were evident: conventional CAR-T cells had a lower expression of the central and stem-cell memory marker CD62L (Figures 6C and S7A). After stimulation, we observed that conventional CAR-T cells had higher expression of exhaustion molecules and lower CD62L expression (Figure 6D). These changes were more dramatic as the effector-to-target (E:T) ratio decreased. *disLCK*-CAR-T cells had more of a memory phenotype than conventional CAR-T cells, with a larger proportion of the less-differentiated stem cell memory (T_{SCM}: $CD45RA^+CD62L^+$) and central memory (T_{cm}: $CD45RA^-CD62L^+$) T cells (Figure 6E). The induction of enhanced memory and

Figure 5. LCK-disrupted CAR-T cells enhance *in vivo* therapeutic efficacy

(A) Cytokine secretion of *disLCK*-CAR-T and conventional CAR-T (generated by lentivirus transduction) upon activation by target cells. The left panel is the representative FACS data, and the right panel is the analytical summary.

(B) Comparison of cytotoxicity of *disLCK*-CAR-T and conventional CAR-T to CD19 expressing Daudi cells at a serial E:T ratio.

(C) Real-time killing curve of *disLCK*-CAR and conventional CAR-T to CHO cells overexpressing CD19. Cell index represents the cell growth. Arrow points show when the CAR-T cells were added. The respective E:T ratio is indicated in parentheses.

(D) Schematic of *in vivo* mouse model of liquid cancer or solid tumor.

(E) Kaplan-Meier analysis of survival in standard leukemia cancer model (Nalm-6 cells and CAR-T cells were administered at 0.5×10^6 and 3×10^6 cells, respectively, log rank Mantel-Cox test). The CAR-T cells in left graph were generated as described in (A) (n = 3–4 mice per group) and were generated by lentivirus transduction. The right graph shows treatment with cells containing both shRNA (either non-targeting control [shNTC] or LCK targeting [shLCK]) and CAR expression cassette (n = 7 mice per CAR-T group, n = 4 for control group treated by PBS).

(F) *In vivo* efficacy of anti-solid tumor mouse model. 2×10^6 breast cancer cell line MCF7-HER2 cells were administered subcutaneously (s.c.) at day 0, and 8×10^6 anti-HER2CAR-T cells were administered on day 5. Tumor size was measured and monitored over time (n = 5 mice per group).

Data in (A)–(C) are representative of 3 independent experiments, plotted as mean ± SD of technical triplicates. p values denoted as in the Figure 1 legend using Student's t test for (A) and two-way ANOVA for (B), (C), and (F).

See Figure S5 for additional data.

CellPress
OPEN ACCESS

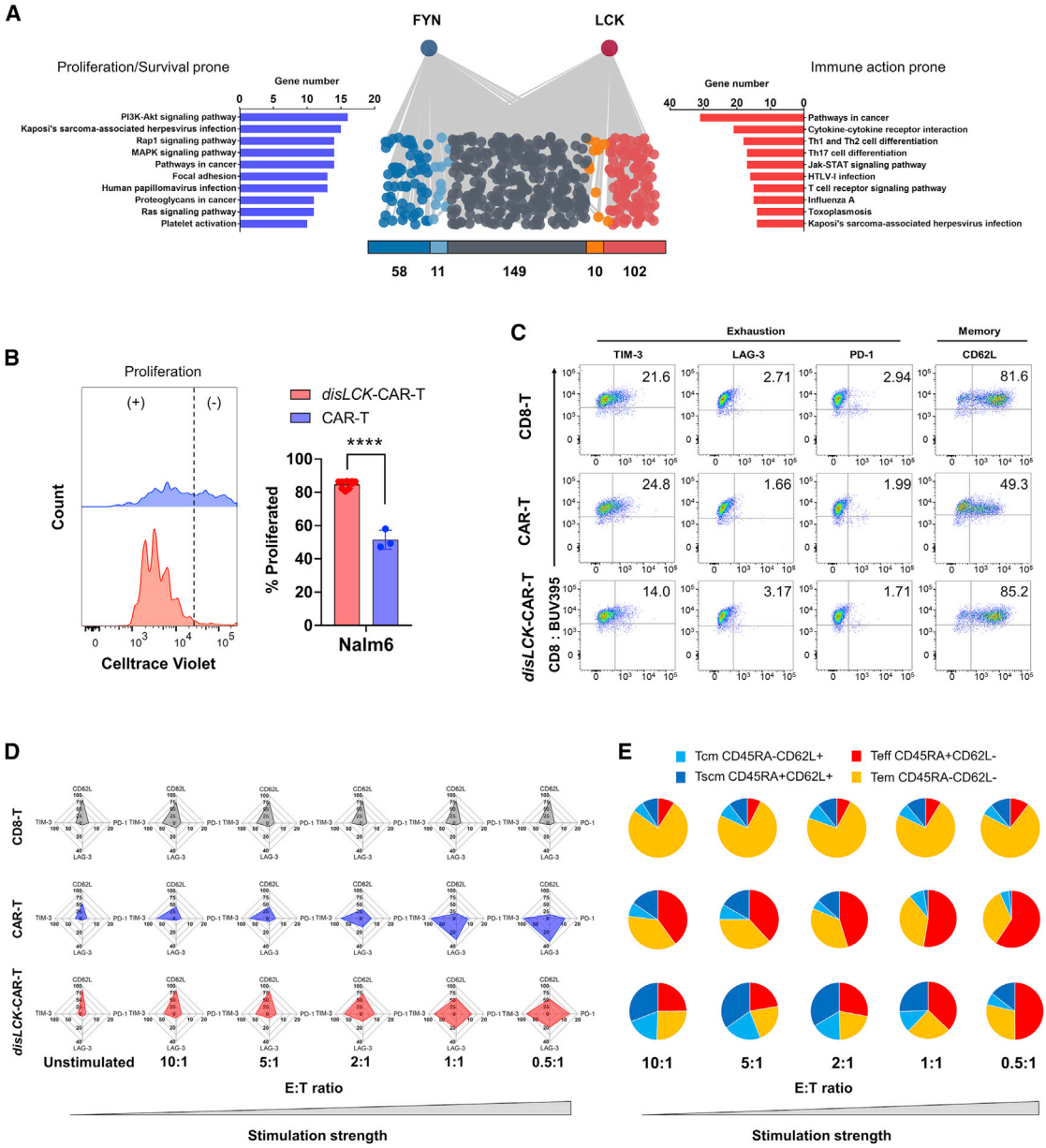

Figure 6. *disLCK*-CAR-T cell activation by FYN leads to a more proliferative, memory-retaining, and exhaustion-reduced state

(A) Signal pathway analysis of FYN and LCK group molecules. The 330 molecules linked to either FYN or LCK can be divided into FYN unique (blue, 58 molecules); FYN more-strongly linked (light blue, 11 molecules); shared linked (dark gray, 149 molecules); LCK more-strongly linked (orange, 10 molecules); and LCK unique (red, 102 molecules). FYN or LCK unique and strongly linked molecules are grouped in the FYN or LCK group, respectively, and analyzed in the KEGG signal pathway database. The pathways are ranked by the number of genes in the respective pathways.

(B) CAR-T cell proliferation upon target cell activation. The proliferation event was detected by FACS after 5-day incubation with Nalm-6 cells. The left panel shows the representative graph, and the right panel is the statistical summary.

(C) CAR, exhaustion, and memory marker expression in resting T cells (5 days after sorting and restimulation by feeder cells).

(D) Radar chart summary of exhaustion, and memory marker expression in T cells after encountering target cells at different E:T ratios. Axes show the percentage of expression of each marker.

(E) Memory subtypes of CAR-T cells after stimulation at different E:T ratios. T cells were stained with anti-CD45RA and anti-CD62L after 18-h incubation with Daudi cells at the corresponding E:T ratio.

Data are representative of 3 (B) or 2 (C–E) independent experiments, plotted as mean ± SD of technical triplicates. p values denoted as in the Figure 1 legend calculated by Student's t test.

See Figures S6 and S7 for additional data.

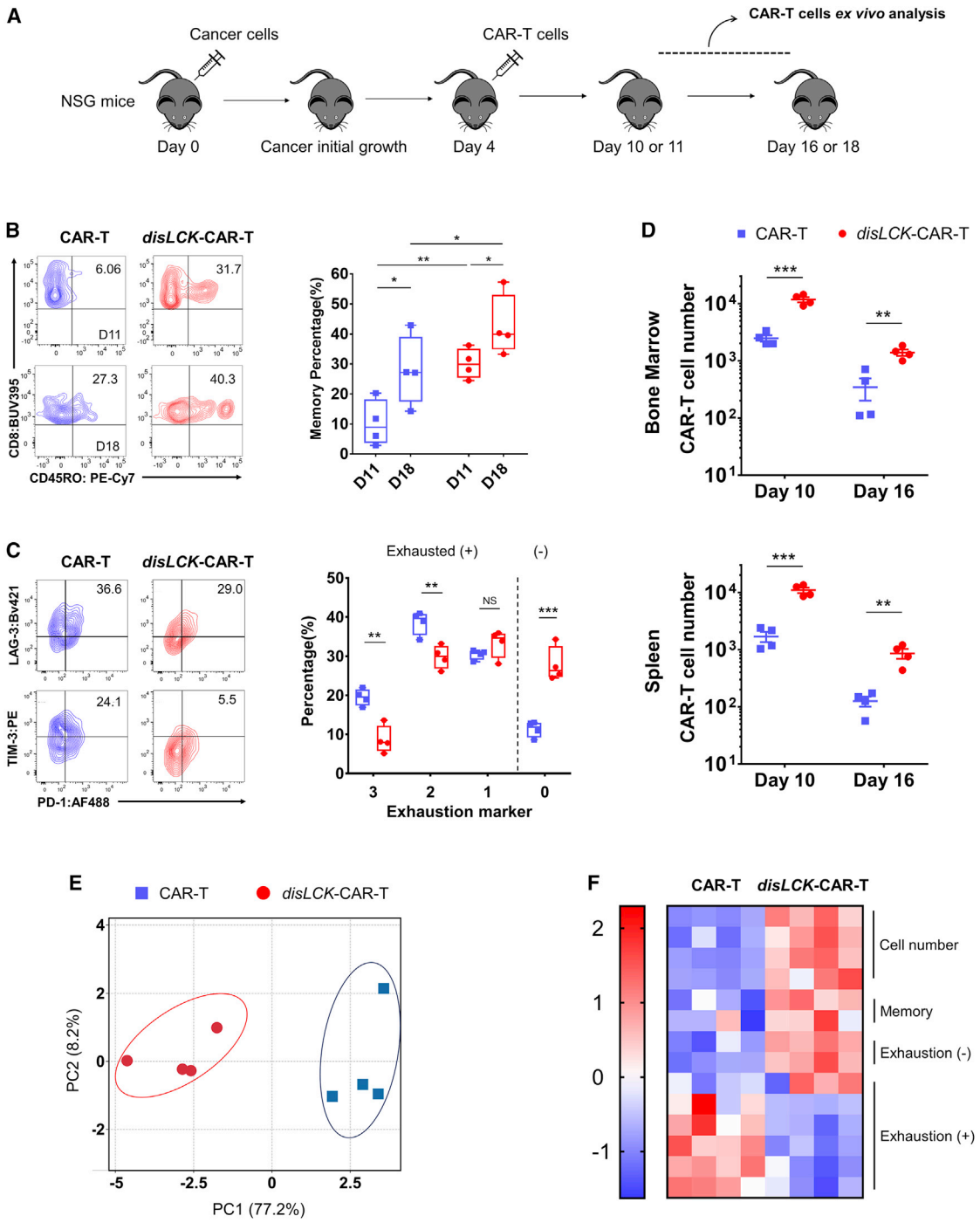

Figure 7. *disLCK*-CAR-T cells have an enhanced therapeutic profile *in vivo*

(A) Schematic of the *ex vivo* analysis of CAR-T cells after administration *in vivo*.

(B) Bone marrow CAR-T cells were analyzed at day 11 or 18 after cancer cells injected, and percentage of memory T cells ($CD45RO^+$) was detected by FACS. The left panel shows the representative FACS data, and the right panel shows the statistical summary. n = 4 mice per group, each dot = one mouse, CAR-T = blue square, *disLCK*-CAR-T = red round dot.

(C) Exhaustion marker expression on the CAR-T cells from bone marrow analyzed on day 10. The left panel shows the representative FACS data, and the right panel shows the statistical summary. n = 4 mice per group, each dot = one mouse, CAR-T = blue square, *disLCK*-CAR-T = red round dot. Cells with 3, 2, or 1 exhaustion marker expression (TIM-3, LAG-3, and PD-1) are designated as exhaustion (+), and cells without exhaustion marker expression are designated as exhaustion (–).

(legend continued on next page)

reduced exhaustion due to targeting the *LCK* gene were verified by comparison with targeting another gene locus: β2-microglobulin (*B2M*). Similar to conventional CAR-T, the *disB2M*-CAR-T cells showed a more differentiated memory state and more exhaustion marker upregulation upon stimulation than *disLCK*-CAR-T cells (Figures S7B–S7E).

disLCK-CAR-T cells have an enhanced therapeutic profile *in vivo*

To reflect the distinct immune-state *in vitro*, *disLCK*-CAR-T and conventional CAR-T cells were immunophenotyped *ex vivo* after administration (Figure 7A). *disLCK*-CAR-T cells showed a significantly higher expression of $CD45RO^+$ memory cells at both days 11 and 18 compared with conventional CAR-T cells (Figure 7B). In addition, conventional CAR-T cells upregulated exhaustion markers PD-1, TIM-3, and LAG3 more than did *disLCK*-CAR-T cells. The percentage of exhaustion marker-negative *disLCK*-CAR-T cells was notably higher than that of conventional CAR-T cells (Figure 7C). Besides this different immunophenotype, the number of *disLCK*-CAR-T cells was significantly higher at days 10 and 16 *in vivo* compared with conventional CAR-T cells (Figures 7D and S7F). We consolidated the *in vivo* performance data and performed principal-component analysis (PCA). *disLCK*-CAR-T and conventional cells can be distinguished as different groups (Figure 7E). *disLCK*-CAR-T cells were enriched in the more persistent, memory-prone, and exhaustion marker-reduced cluster, contrasting significantly with conventional CAR-T cells (Figure 7F). In summary, these data suggest that tilting CD28-CAR-T activation toward FYN via disruption of LCK expression, results in a more proliferative, memory-retaining, and less exhausted phenotype, explaining the enhanced therapeutic performance of *disLCK*-CAR-T cells *in vivo*.

DISCUSSION

Although huge successes have been seen with CAR-T therapy in the clinic, CAR signaling itself has not yet been fully defined.[3] To this end, we intended to identify molecules specifically relevant to CAR, but not TCR, signaling on the basis that this could reveal potentially useful properties specific to CAR signaling. Surprisingly, CAR signaling was triggered normally even in the absence of LCK. In addition, the cytokine release by *disLCK*-CAR-T cells was significantly higher than that of conventional CAR-T cells. This could be related to the signal regulatory function of LCK.[26] On the other hand reduced LCK expression significantly decreases TCR signaling strength,[27] explaining why endogenous TCR signaling was dramatically inhibited in *disLCK*-CAR-T cells. This trait of splitting CAR and TCR signal activation in the absence of LCK could be exploited to generate allogeneic CAR-T. Unlike knocking out TCR in CAR-T cells, which results in lower persistence *in vivo,*[28] TCR-retaining *disLCK*-CAR-T cells could potentially sustain tonic signaling, thus prolonging survival of allogeneic CAR-T cells.[29] This point could be inferred from our observation that ERK in LCK-deficient TCR-T cells was phosphorylated upon stimulation by pMHC, perhaps due to a PLCγ1-independent signaling pathway.[30,31]

This non-canonical CAR signaling pathway has not previously been reported in CAR-T studies. Systematic scrutinization of CAR domains revealed that the CD28 co-stimulatory domain plays a critical role. FYN, the other SFK active in T cell signaling, has been shown to bind to TCR in proximal signaling.[32,33] It could also be important in non-canonical CAR signaling. Deletion of FYN or LCK in Jurkat cells using CRISPR-Cas9 showed that CAR signaling relies more on FYN than on LCK. Despite the limitations of Jurkat cells, proximal TCR signaling mechanisms in Jurkat resemble those in primary T cells.[23,24] Hence, these results suggested that FYN could be the major kinase orchestrating CAR signal transduction under physiological conditions. We showed that LCK-independent CAR signaling is mediated by the interplay between FYN and the CD28 domain. The role of CD28 in CAR is not primarily related to a spacer effect—by which CD3ζ is distanced from the cell membrane—because this spacer effect was not sufficient to trigger LCK-independent signaling for CD137-CAR, and the reduction of LCK-independent CAR signaling was observed with point mutations in CD28. Nonetheless, the spacer effect may make CD3ζ more accessible to FYN compared with LCK. FYN is localized more freely than LCK, including association with the endoplasmic reticulum (ER) or cytoskeleton.[34–37] This could favor CD3ζ phosphorylation by FYN given that CD3ζ is the preferred substrate for FYN, whereas LCK preferentially phosphorylates CD3ε.[24] We attribute LCK-independent CAR signaling primarily to signal functions of the CD28 module, such as the FYN recruitment by CD28 shown in this study. This could explain why the third-generation CAR showed LCK-independent signaling, but to a limited degree, where CD28 signaling was disrupted when the CD137 domain was between CD28 and CD3ζ domains. The importance of the transmembrane has not been explored in this study, but it may play a role in mediating the LCK-independent CAR signaling to a certain degree given that it has been reported to influence downstream CAR signaling.[38] Interestingly, first-generation CAR or TCR, as well as CD137-CAR, was able to resume signal activation in the absence of LCK when endogenous CD28 was co-stimulated in *trans*. Based on our findings, we hypothesize that CD28 may bring FYN to the IS once co-stimulated, partially to fulfill LCK's function. The kinase switch in CD28-containing CAR compared with CD137-containing CAR potentially explains their distinct performances as seen in previous studies,[20,27,37]

(D) Cell number of the CAR-T cells from bone marrow and spleen at days 10 and 16 after cancer cells were injected. 1.8×10^6 CAR-T cells were administered in each mouse at day 4 after 1.5×10^6 Nalm-6 cells were injected at day 0. n = 4 mice per group.

(E) Principal-component analysis (PCA) of conventional CAR-T and *disLCK*-CAR-T cell *in vivo* performance. Each dot = one mouse, *disLCK*-CAR-T = red round dots, conventional CAR-T = blue square dots.

(F) Heatmap of the *in vivo* performances of CAR-T cells after PCA. The columns are biological repeats. Each row represents PCA values of *ex vivo* data of each factor, memory is the $CD45RO^+$ group, and exhaustion (−) and (+) are defined the same as in (C).

Data in (B)–(D) are means ± SD. Boxes in (B) (right panels) represent 95% confidence intervals. p values denoted as in the Figure 1 legend using Student's t test. See Figure S7F for additional data.

FYN and LCK are distinct in terms of signaling kinetics, pathways, and strength. FYN-mediated CD28-CAR signaling would, therefore, show different responses than CD137-CAR signaling, where their initiations are controlled by different kinases. Although CD28 co-stimulatory signaling has been studied intensively, it has seldom been explored under LCK-deficient conditions.[18] Since LCK and FYN have both been shown to interact with CD28,[39] CD28 signaling might be different when only FYN can interact with it. However, to what degree the CD28 co-stimulatory signaling pathways, such as the PI3K, PKCθ, and AKT pathways, have been affected after disruption of LCK is unknown.

The balance of FYN and LCK in T cells could naturally favor FYN signaling after LCK disruption, resulting in a favorable therapeutic performance that increases the overall *in vivo* efficacy. FYN and LCK both have uniquely linked and more-strongly linked molecules (FYN or LCK group) in TCR signaling. Signal pathway analysis reveals that the interactions within the FYN-specific group would provide T cells with the tendency to proliferate and survive. This analysis is consistent with previous studies on FYN where FYN controls cell growth.[40,41] On the other hand, the LCK-specific signaling partners are more relevant in immune activity. It is likely that CAR-T cells with LCK present are more easily overactivated and thus exhausted. For example, overactivated and chronic nuclear factor κB (NF-κB) signaling—which is more involved in the LCK-unique system in T cells—would lead to cellular senescence and apoptosis.[42,43] This could be important for CD28-CAR-T cells, which may be chronically activated, leading to early exhaustion.[44] Treating CD28-CAR-T cells with the LCK inhibitor dasatinib during culture or changing to a CD137 co-stimulatory domain, which would recruit THEMIS-SHP1 to inhibit LCK activity, could avoid early exhaustion.[9,45] Dasatinib, however, has broad inhibition of the SFK and other kinases, including both LCK and FYN. This could obscure the fact identified in this study that FYN could be more important to CD28-CAR. Nevertheless, it will not affect its application to control CAR signaling and as a pharmacological switch since LCK and FYN are both inhibited by using dasatinib.[46] Overall, *disLCK*-CAR-T cells became more proliferative, showed resistance to exhaustion, and tended to retain memory phenotype, leading to their increased *in vivo* efficacy and suggesting significant benefits for translation in clinical settings.

In conclusion, we report that CAR-T signaling can be triggered without the presence of LCK. We show that this non-canonical signaling pathway bypassing LCK is related to the CD28 co-stimulatory domain. Moreover, FYN is revealed to be more crucial than LCK in CD28-CAR signal transduction. This kinase switch provides distinct properties for *disLCK*-CAR-T cells, including tolerance to inhibitory signals and a propensity to proliferate and differentiate to memory cells. The *disLCK*-CAR-T cells could provide a more durable and effective CAR-T therapy for clinical use and suggest that editing signaling molecules may be a fruitful avenue to construct the next generation of CAR-T technologies.

Limitations of the study

The study primarily focuses on $CD8^+$ T cells. $CD4^+$ T cells were not part of the study. Although LCK-independent CAR signaling should be replicable, the impact to $CD4^+$-CAR-T cells could be different compared with $CD8^+$-CAR-T cells. Future studies should include both $CD4^+$ and $CD8^+$ T cells. In addition, omics studies such as transcriptome and phosphoproteomics were not performed. With the disruption of LCK in CAR-T cells, cell fate and signaling associated with CD28 co-stimulatory signaling after activation could be distinct. A better understanding of the *disLCK*-CAR-T cells can be acquired after such omics studies.

STAR★METHODS

Detailed methods are provided in the online version of this paper and include the following:

- KEY RESOURCES TABLE
- RESOURCE AVAILABILITY
  - Lead contact
  - Materials availability
  - Data and code availability
- EXPERIMENTAL MODEL AND SUBJECT DETAILS
  - Cell lines and cell culture
  - Primary $CD8^+$ T cell activation and culture
  - *In vivo* animal model
- METHOD DETAILS
  - Constructs and sequences
  - Lentivirus production and transduction
  - CRISPR-Cas9 knock-out and knock-in genetic editing
  - Calcium flux assay
  - T cell stimulation and cytokine secretion assay
  - Cytotoxicity assay
  - Western blotting and immunoprecipitation (IP)
  - Flow cytometry and cell sorting
  - Signal pathway analysis
  - Statistical information and data analysis

SUPPLEMENTAL INFORMATION

Supplemental information can be found online at https://doi.org/10.1016/j.xcrm.2023.100917.

ACKNOWLEDGMENTS

We thank the flow cytometry core facility team of The Life Sciences Institute (LSI), NUS, for sorting and Professors Hans Stauss, Antonio Bertoletti, and Keith Gould for providing TCR and scHLA constructs; Professors Dario Campana and Haiyan Liu for support and helpful suggestions on animal studies; and Dr. Gan Shu Uin for helpful suggestions on virus production. This work was funded by NUS ILO TAP grant TAP2002019-04-25, Singapore Ministry of Health's National Medical Research Council MOH-000523, and Ministry of Education NUHSRO/2020/110/T1/SEED-MAR/06. L.W., Q.W., and J.L. were supported by research scholarships from Yong Loo Lin School of Medicine.

AUTHOR CONTRIBUTIONS

L.W. designed, conducted experiments, and analyzed the data; J.B. and N.R.J.G. provided discussion and co-designed experiments; Q.W. provided discussion and support on LCK analysis; P.D.S.V., J.X.H.O., L.-z.W., Y.S., J.C.T., J.Y., V.J.Y.T., Y.L.C., and T.Y.Y.T. provided technical or practical help; C.K.T.K. prepared the TCR signal molecule pool for bioinformatic

analysis. J.L. and P.A.M. provided Ab sequences and reagents; and L.W., J.B., and N.R.J.G. wrote the paper with input and final approval from all authors.

DECLARATION OF INTERESTS

National University of Singapore has filed patents based on these findings. P.A.M. is a shareholder and advisory board member of Gen Y Biologics Pte., Ltd. (company registration number: 202005553Z). Patent title: Engineered Immune Cells (PCT/SG2020/050090). Published September 10, 2020: WO 2020/180243 (L.W., N.R.J.G., and J.B.).

INCLUSION AND DIVERSITY

We support inclusive, diverse, and equitable conduct of research.

Received: July 24, 2022
Revised: September 7, 2022
Accepted: January 4, 2023
Published: January 24, 2023

REFERENCES

1. Kochenderfer, J.N., Yu, Z., Frasheri, D., Restifo, N.P., and Rosenberg, S.A. (2010). Adoptive transfer of syngeneic T cells transduced with a chimeric antigen receptor that recognizes murine CD19 can eradicate lymphoma and normal B cells. Blood *116*, 3875–3886. https://doi.org/10.1182/blood-2010-01-265041.
2. Kalos, M., Levine, B.L., Porter, D.L., Katz, S., Grupp, S.A., Bagg, A., and June, C.H. (2011). T cells with chimeric antigen receptors have potent antitumor effects and can establish memory in patients with advanced leukemia. Sci. Transl. Med. *3*, 95ra73. https://doi.org/10.1126/scitranslmed.3002842.
3. Wu, L., Wei, Q., Brzostek, J., and Gascoigne, N.R.J. (2020). Signaling from T cell receptors (TCRs) and chimeric antigen receptors (CARs) on T cells. Cell. Mol. Immunol. *17*, 600–612. https://doi.org/10.1038/s41423-020-0470-3.
4. Salter, A.I., Ivey, R.G., Kennedy, J.J., Voillet, V., Rajan, A., Alderman, E.J., Voytovich, U.J., Lin, C., Sommermeyer, D., Liu, L., et al. (2018). Phosphoproteomic analysis of chimeric antigen receptor signaling reveals kinetic and quantitative differences that affect cell function. Sci. Signal. *11*, eaat6753. https://doi.org/10.1126/scisignal.aat6753.
5. Davenport, A.J., Cross, R.S., Watson, K.A., Liao, Y., Shi, W., Prince, H.M., Beavis, P.A., Trapani, J.A., Kershaw, M.H., Ritchie, D.S., et al. (2018). Chimeric antigen receptor T cells form nonclassical and potent immune synapses driving rapid cytotoxicity. Proc. Natl. Acad. Sci. USA *115*, E2068–E2076. https://doi.org/10.1073/pnas.1716266115.
6. Gulati, P., Rühl, J., Kannan, A., Pircher, M., Schuberth, P., Nytko, K.J., Pruschy, M., Sulser, S., Haefner, M., Jensen, S., et al. (2018). Aberrant lck signal via CD28 costimulation augments antigen-specific functionality and tumor control by redirected T cells with PD-1 blockade in humanized mice. Clin. Cancer Res. *24*, 3981–3993. https://doi.org/10.1158/1078-0432.CCR-17-1788.
7. Xiong, W., Chen, Y., Kang, X., Chen, Z., Zheng, P., Hsu, Y.H., Jang, J.H., Qin, L., Liu, H., Dotti, G., and Liu, D. (2018). Immunological synapse predicts effectiveness of chimeric antigen receptor cells. Mol. Ther. *26*, 963–975. https://doi.org/10.1016/j.ymthe.2018.01.020.
8. Rohrs, J.A., Zheng, D., Graham, N.A., Wang, P., and Finley, S.D. (2018). Computational model of chimeric antigen receptors explains site-specific phosphorylation kinetics. Biophys. J. *115*, 1116–1129. https://doi.org/10.1016/j.bpj.2018.08.018.
9. Sun, C., Shou, P., Du, H., Hirabayashi, K., Chen, Y., Herring, L.E., Ahn, S., Xu, Y., Suzuki, K., Li, G., et al. (2020). THEMIS-SHP1 recruitment by 4-1BB tunes LCK-mediated priming of chimeric antigen receptor-redirected T cells. Cancer Cell *37*, 216–225.e6. https://doi.org/10.1016/j.ccell.2019.12.014.
10. Molina, T.J., Kishihara, K., Siderovski, D.P., van Ewijk, W., Narendran, A., Timms, E., Wakeham, A., Paige, C.J., Hartmann, K.U., Veillette, A., et al. (1992). Profound block in thymocyte development in mice lacking p56lck. Nature *357*, 161–164. https://doi.org/10.1038/357161a0.
11. Straus, D.B., and Weiss, A. (1992). Genetic evidence for the involvement of the lck tyrosine kinase in signal transduction through the T cell antigen receptor. Cell *70*, 585–593.
12. Lai, J., Choo, J.A.L., Tan, W.J., Too, C.T., Oo, M.Z., Suter, M.A., Mustafa, F.B., Srinivasan, N., Chan, C.E.Z., Lim, A.G.X., et al. (2017). TCR-like antibodies mediate complement and antibody-dependent cellular cytotoxicity against Epstein-Barr virus-transformed B lymphoblastoid cells expressing different HLA-A*02 microvariants. Sci. Rep. *7*, 9923. https://doi.org/10.1038/s41598-017-10265-6.
13. Sim, A.C.N., Too, C.T., Oo, M.Z., Lai, J., Eio, M.Y., Song, Z., Srinivasan, N., Tan, D.A.L., Pang, S.W., Gan, S.U., et al. (2013). Defining the expression hierarchy of latent T-cell epitopes in Epstein-Barr virus infection with TCR-like antibodies. Sci. Rep. *3*, 3232. https://doi.org/10.1038/srep03232.
14. Wu, L., Brzostek, J., Sankaran, S., Wei, Q., Yap, J., Tan, T.Y.Y., Lai, J., MacAry, P.A., and Gascoigne, N.R.J. (2021). Targeting CAR to the peptide-MHC complex reveals distinct signaling compared to that of TCR in a Jurkat T cell model. Cancers *13*, 867. https://doi.org/10.3390/cancers13040867.
15. Banik, D., Hamidinia, M., Brzostek, J., Wu, L., Stephens, H.M., MacAry, P.A., Reinherz, E.L., Gascoigne, N.R.J., and Lang, M.J. (2021). Single molecule force spectroscopy reveals distinctions in key biophysical parameters of alphabeta T-cell receptors compared with chimeric antigen receptors directed at the same ligand. J. Phys. Chem. Lett. *12*, 7566–7573. https://doi.org/10.1021/acs.jpclett.1c02240.
16. Gascoigne, N.R.J., Casas, J., Brzostek, J., and Rybakin, V. (2011). Initiation of TCR phosphorylation and signal transduction. Front. Immunol. *2*, 72. https://doi.org/10.3389/fimmu.2011.00072.
17. Artyomov, M.N., Lis, M., Devadas, S., Davis, M.M., and Chakraborty, A.K. (2010). CD4 and CD8 binding to MHC molecules primarily acts to enhance Lck delivery. Proc. Natl. Acad. Sci. USA *107*, 16916–16921. https://doi.org/10.1073/pnas.1010568107.
18. Esensten, J.H., Helou, Y.A., Chopra, G., Weiss, A., and Bluestone, J.A. (2016). CD28 costimulation: from mechanism to therapy. Immunity *44*, 973–988. https://doi.org/10.1016/j.immuni.2016.04.020.
19. Moeller, M., Haynes, N.M., Trapani, J.A., Teng, M.W.L., Jackson, J.T., Tanner, J.E., Cerutti, L., Jane, S.M., Kershaw, M.H., Smyth, M.J., and Darcy, P.K. (2004). A functional role for CD28 costimulation in tumor recognition by single-chain receptor-modified T cells. Cancer Gene Ther. *11*, 371–379. https://doi.org/10.1038/sj.cgt.7700710.
20. Palacios, E.H., and Weiss, A. (2004). Function of the src-family kinases, lck and fyn, in T-cell development and activation. Oncogene *23*, 7990–8000. https://doi.org/10.1038/sj.onc.1208074.
21. Blake, R.A., Broome, M.A., Liu, X., Wu, J., Gishizky, M., Sun, L., and Courtneidge, S.A. (2000). SU6656, a selective src family kinase inhibitor, used to probe growth factor signaling. Mol. Cell Biol. *20*, 9018–9027. https://doi.org/10.1128/mcb.20.23.9018-9027.2000.
22. Stachlewitz, R.F., Hart, M.A., Bettencourt, B., Kebede, T., Schwartz, A., Ratnofsky, S.E., Calderwood, D.J., Waegell, W.O., and Hirst, G.C. (2005). A-770041, a novel and selective small-molecule inhibitor of Lck, prevents heart allograft rejection. J. Pharmacol. Exp. Ther. *315*, 36–41. https://doi.org/10.1124/jpet.105.089169.
23. Abraham, R.T., and Weiss, A. (2004). Jurkat T cells and development of the T-cell receptor signalling paradigm. Nat. Rev. Immunol. *4*, 301–308. https://doi.org/10.1038/nri1330.
24. Li, L., Guo, X., Shi, X., Li, C., Wu, W., Yan, C., Wang, H., Li, H., and Xu, C. (2017). Ionic CD3-Lck interaction regulates the initiation of T-cell receptor signaling. Proc. Natl. Acad. Sci. USA *114*, E5891–E5899. https://doi.org/10.1073/pnas.1701990114.

25. Sastry, K.S.R., Too, C.T., Kaur, K., Gehring, A.J., Low, L., Javiad, A., Pollicino, T., Li, L., Kennedy, P.T.F., Lopatin, U., et al. (2011). Targeting hepatitis B virus-infected cells with a T-cell receptor-like antibody. J. Virol. *85*, 1935–1942. https://doi.org/10.1128/JVI.01990-10.

26. Salmond, R.J., Filby, A., Qureshi, I., Caserta, S., and Zamoyska, R. (2009). T-cell receptor proximal signaling via the Src-family kinases, Lck and Fyn, influences T-cell activation, differentiation, and tolerance. Immunol. Rev. *228*, 9–22. https://doi.org/10.1111/j.1600-065X.2008.00745.x.

27. Denny, M.F., Patai, B., and Straus, D.B. (2000). Differential T-cell antigen receptor signaling mediated by the Src family kinases Lck and Fyn. Mol. Cell Biol. *20*, 1426–1435.

28. Stenger, D., Stief, T.A., Kaeuferle, T., Willier, S., Rataj, F., Schober, K., Vick, B., Lotfi, R., Wagner, B., Grünewald, T.G.P., et al. (2020). Endogenous TCR promotes in vivo persistence of CD19-CAR-T cells compared to a CRISPR/Cas9-mediated TCR knockout CAR. Blood *136*, 1407–1418. https://doi.org/10.1182/blood.2020005185.

29. Seddon, B., Legname, G., Tomlinson, P., and Zamoyska, R. (2000). Long-term survival but impaired homeostatic proliferation of Naive T cells in the absence of p56lck. Science *290*, 127–131. https://doi.org/10.1126/science.290.5489.127.

30. Shan, X., Balakir, R., Criado, G., Wood, J.S., Seminario, M.C., Madrenas, J., and Wange, R.L. (2001). Zap-70-independent Ca(2+) mobilization and Erk activation in Jurkat T cells in response to T-cell antigen receptor ligation. Mol. Cell Biol. *21*, 7137–7149. https://doi.org/10.1128/MCB.21.21.7137-7149.2001.

31. Kortum, R.L., Rouquette-Jazdanian, A.K., Miyaji, M., Merrill, R.K., Markegard, E., Pinski, J.M., Wesselink, A., Nath, N.N., Alexander, C.P., Li, W., et al. (2013). A phospholipase C-gamma1-independent, RasGRP1-ERK-dependent pathway drives lymphoproliferative disease in linker for activation of T cells-Y136F mutant mice. J. Immunol. *190*, 147–158. https://doi.org/10.4049/jimmunol.1201458.

32. Gauen, L.K., Zhu, Y., Letourneur, F., Hu, Q., Bolen, J.B., Matis, L.A., Klausner, R.D., and Shaw, A.S. (1994). Interactions of p59fyn and ZAP-70 with T-cell receptor activation motifs: defining the nature of a signalling motif. Mol. Cell Biol. *14*, 3729–3741. https://doi.org/10.1128/mcb.14.6.3729-3741.1994.

33. Samelson, L.E., Phillips, A.F., Luong, E.T., and Klausner, R.D. (1990). Association of the fyn protein-tyrosine kinase with the T-cell antigen receptor. Proc. Natl. Acad. Sci. USA *87*, 4358–4362. https://doi.org/10.1073/pnas.87.11.4358.

34. Ley, S.C., Marsh, M., Bebbington, C.R., Proudfoot, K., and Jordan, P. (1994). Distinct intracellular localization of Lck and Fyn protein tyrosine kinases in human T lymphocytes. J. Cell Biol. *125*, 639–649.

35. Frasson, M., Vitadello, M., Brunati, A.M., La Rocca, N., Tibaldi, E., Pinna, L.A., Gorza, L., and Donella-Deana, A. (2009). Grp94 is Tyr-phosphorylated by Fyn in the lumen of the endoplasmic reticulum and translocates to Golgi in differentiating myoblasts. Biochim. Biophys. Acta *1793*, 239–252. https://doi.org/10.1016/j.bbamcr.2008.10.001.

36. Liang, J., Lyu, J., Zhao, M., Li, D., Zheng, M., Fang, Y., Zhao, F., Lou, J., Guo, C., Wang, L., et al. (2017). Tespa1 regulates T cell receptor-induced calcium signals by recruiting inositol 1,4,5-trisphosphate receptors. Nat. Commun. *8*, 15732. https://doi.org/10.1038/ncomms15732.

37. Lovatt, M., Filby, A., Parravicini, V., Werlen, G., Palmer, E., and Zamoyska, R. (2006). Lck regulates the threshold of activation in primary T cells, while both Lck and Fyn contribute to the magnitude of the extracellular signal-related kinase response. Mol. Cell Biol. *26*, 8655–8665. https://doi.org/10.1128/MCB.00168-06.

38. Majzner, R.G., Rietberg, S.P., Sotillo, E., Dong, R., Vachharajani, V.T., Labanieh, L., Myklebust, J.H., Kadapakkam, M., Weber, E.W., Tousley, A.M., et al. (2020). Tuning the antigen density requirement for CAR T-cell activity. Cancer Discov. *10*, 702–723. https://doi.org/10.1158/2159-8290.CD-19-0945.

39. Raab, M., Cai, Y.C., Bunnell, S.C., Heyeck, S.D., Berg, L.J., and Rudd, C.E. (1995). p56Lck and p59Fyn regulate CD28 binding to phosphatidylinositol 3-kinase, growth factor receptor-bound protein GRB-2, and T cell-specific protein-tyrosine kinase ITK: implications for T-cell costimulation. Proc. Natl. Acad. Sci. USA *92*, 8891–8895. https://doi.org/10.1073/pnas.92.19.8891.

40. Posadas, E.M., Al-Ahmadie, H., Robinson, V.L., Jagadeeswaran, R., Otto, K., Kasza, K.E., Tretiakov, M., Siddiqui, J., Pienta, K.J., Stadler, W.M., et al. (2009). FYN is overexpressed in human prostate cancer. BJU Int. *103*, 171–177. https://doi.org/10.1111/j.1464-410X.2008.08009.x.

41. Saito, Y.D., Jensen, A.R., Salgia, R., and Posadas, E.M. (2010). Fyn: a novel molecular target in cancer. Cancer *116*, 1629–1637. https://doi.org/10.1002/cncr.24879.

42. Zhi, H., Yang, L., Kuo, Y.L., Ho, Y.K., Shih, H.M., and Giam, C.Z. (2011). NF-kappaB hyper-activation by HTLV-1 tax induces cellular senescence, but can be alleviated by the viral anti-sense protein HBZ. PLoS Pathog. *7*, e1002025. https://doi.org/10.1371/journal.ppat.1002025.

43. Krishna, S., Xie, D., Gorentla, B., Shin, J., Gao, J., and Zhong, X.P. (2012). Chronic activation of the kinase IKKbeta impairs T cell function and survival. J. Immunol. *189*, 1209–1219. https://doi.org/10.4049/jimmunol.1102429.

44. Long, A.H., Haso, W.M., Shern, J.F., Wanhainen, K.M., Murgai, M., Ingaramo, M., Smith, J.P., Walker, A.J., Kohler, M.E., Venkateshwara, V.R., et al. (2015). 4-1BB costimulation ameliorates T cell exhaustion induced by tonic signaling of chimeric antigen receptors. Nat. Med. *21*, 581–590. https://doi.org/10.1038/nm.3838.

45. Weber, E.W., Parker, K.R., Sotillo, E., Lynn, R.C., Anbunathan, H., Lattin, J., Good, Z., Belk, J.A., Daniel, B., Klysz, D., et al. (2021). Transient rest restores functionality in exhausted CAR-T cells through epigenetic remodeling. Science *372*, eaba1786. https://doi.org/10.1126/science.aba1786.

46. Mestermann, K., Giavridis, T., Weber, J., Rydzek, J., Frenz, S., Nerreter, T., Mades, A., Sadelain, M., Einsele, H., and Hudecek, M. (2019). The tyrosine kinase inhibitor dasatinib acts as a pharmacologic on/off switch for CAR T cells. Sci. Transl. Med. *11*, eaau5907. https://doi.org/10.1126/scitranslmed.aau5907.

47. Heemskerk, M.H.M., Hoogeboom, M., de Paus, R.A., Kester, M.G.D., van der Hoorn, M.A.W.G., Goulmy, E., Willemze, R., and Falkenburg, J.H.F. (2003). Redirection of antileukemic reactivity of peripheral T lymphocytes using gene transfer of minor histocompatibility antigen HA-2-specific T-cell receptor complexes expressing a conserved alpha joining region. Blood *102*, 3530–3540. https://doi.org/10.1182/blood-2003-05-1524.

48. Methi, T., Ngai, J., Mahic, M., Amarzguioui, M., Vang, T., and Tasken, K. (2005). Short-interfering RNA-mediated Lck knockdown results in augmented downstream T cell responses. J. Immunol. *175*, 7398–7406. https://doi.org/10.4049/jimmunol.175.11.7398.

49. Sarbassov, D.D., Guertin, D.A., Ali, S.M., and Sabatini, D.M. (2005). Phosphorylation and regulation of Akt/PKB by the rictor-mTOR complex. Science *307*, 1098–1101. https://doi.org/10.1126/science.1106148.

50. Jena, B., Maiti, S., Huls, H., Singh, H., Lee, D.A., Champlin, R.E., and Cooper, L.J.N. (2013). Chimeric antigen receptor (CAR)-specific monoclonal antibody to detect CD19-specific T cells in clinical trials. PLoS One *8*, e57838. https://doi.org/10.1371/journal.pone.0057838.

51. Zhao, Y., Wang, Q.J., Yang, S., Kochenderfer, J.N., Zheng, Z., Zhong, X., Sadelain, M., Eshhar, Z., Rosenberg, S.A., and Morgan, R.A. (2009). A herceptin-based chimeric antigen receptor with modified signaling domains leads to enhanced survival of transduced T lymphocytes and antitumor activity. J. Immunol. *183*, 5563–5574. https://doi.org/10.4049/jimmunol.0900447.

52. Hoerter, J.A.H., Brzostek, J., Artyomov, M.N., Abel, S.M., Casas, J., Rybakin, V., Ampudia, J., Lotz, C., Connolly, J.M., Chakraborty, A.K., et al. (2013). Coreceptor affinity for MHC defines peptide specificity requirements for TCR interaction with coagonist peptide-MHC. J. Exp. Med. *210*, 1807–1821. https://doi.org/10.1084/jem.20122528.

53. Zhao, X., Sankaran, S., Yap, J., Too, C.T., Ho, Z.Z., Dolton, G., Legut, M., Ren, E.C., Sewell, A.K., Bertoletti, A., et al. (2018). Nonstimulatory peptide-MHC enhances human T-cell antigen-specific responses by amplifying

proximal TCR signaling. Nat. Commun. *9*, 2716. https://doi.org/10.1038/s41467-018-05288-0.

54. Zhao, X., Hamidinia, M., Choo, J.A.L., Too, C.T., Ho, Z.Z., Ren, E.C., Bertoletti, A., MacAry, P.A., Gould, K.G., Brzostek, J., and Gascoigne, N.R.J. (2019). Use of single chain MHC technology to investigate Co-agonism in human CD8+ T cell activation. J. Vis. Exp. https://doi.org/10.3791/59126.
55. Sanjana, N.E., Shalem, O., and Zhang, F. (2014). Improved vectors and genome-wide libraries for CRISPR screening. Nat. Methods *11*, 783–784. https://doi.org/10.1038/nmeth.3047.
56. Roth, T.L., Puig-Saus, C., Yu, R., Shifrut, E., Carnevale, J., Li, P.J., Hiatt, J., Saco, J., Krystofinski, P., Li, H., et al. (2018). Reprogramming human T cell function and specificity with non-viral genome targeting. Nature *559*, 405–409. https://doi.org/10.1038/s41586-018-0326-5.
57. Fu, G., and Gascoigne, N.R.J. (2009). Multiplexed labeling of samples with cell tracking dyes facilitates rapid and accurate internally controlled calcium flux measurement by flow cytometry. J. Immunol. Methods *350*, 194–199. https://doi.org/10.1016/j.jim.2009.07.009.
58. Choo, J.A.L., Thong, S.Y., Yap, J., van Esch, W.J.E., Raida, M., Meijers, R., Lescar, J., Verhelst, S.H.L., and Grotenbreg, G.M. (2014). Bioorthogonal cleavage and exchange of major histocompatibility complex ligands by employing azobenzene-containing peptides. Angew. Chem. Int. Ed. Engl. *53*, 13390–13394. https://doi.org/10.1002/anie.201406295.

STAR★METHODS

KEY RESOURCES TABLE

REAGENT or RESOURCE	SOURCE	IDENTIFIER
Antibodies		
Myc-Tag (9B11) Mouse mAb (PE Conjugate)	Cell Signaling Technology	Cat# 3739S; RRID:AB_10889248
Myc-Tag (71D10) Rabbit mAb (Alexa Fluor® 700 Conjugate)	Cell Signaling Technology	Cat# 42136S; RRID:AB_2799214
Myc-Tag (9B11) Mouse mAb (Alexa Fluor® 647 Conjugate)	Cell Signaling Technology	Cat# 2233S; RRID:AB_823474
Phospho-Src Family (Tyr416) (D49G4) Rabbit mAb	Cell Signaling Technology	Cat# 6943S; RRID:AB_10013641
Phospho-PLCγ1 (Tyr783) Antibody	Cell Signaling Technology	Cat# 2821S; RRID:AB_330855
Phospho p44/42 MAPK (Erk1) (Tyr204)/(Erk2) (Tyr187) (D1H6G) Mouse mAb	Cell Signaling Technology	Cat# 5726S; RRID:AB_2797617
Phospho-CD3ζ (Tyr142) Antibody	Cell Signaling Technology	Cat# 67748S
c-Cbl Antibody	Cell Signaling Technology	Cat# 2747S; RRID:AB_2275284
PLC-γ1 Antibody	Cell Signaling Technology	Cat# 2822S; RRID:AB_2163702
Purified Mouse Anti-ERK1 Clone MK12 (RUO)	BD Biosciences	Cat# 610031; RRID:AB_397448
Anti-Human CD8 BUV395	BD Biosciences	Cat# 563795; RRID:AB_2722501
BV421 Mouse Anti-Human IFN-γ	BD Biosciences	Cat# 562988; RRID:AB_2737934
Purified anti-Fyn [FYN-59]	Biolegend	Cat# 626502; RRID:AB_2278824
Anti-Human CD28 Alexa 488	Biolegend	Cat# 302916; RRID:AB_493100
PE anti-human CD80 [2D10]	Biolegend	Cat# 305207; RRID:AB_314503
FITC anti-human CD19 [4G7]	Biolegend	Cat# 392507; RRID:AB_2750098
Brilliant Violet 421™ anti-human CD86 Antibody	Biolegend	Cat# 374211; RRID:AB_2728393
APC anti-human CD3 [OKT3]	Biolegend	Cat# 317318; RRID:AB_1937212
PE anti-human CD279 (PD-1) Antibody	Biolegend	Cat# 329905; RRID:AB_940481
Brilliant Violet 711™ anti-human CD279 (PD-1) Antibody	Biolegend	Cat# 367427; RRID:AB_2721554
Fluor® 488 anti-human CD279 (PD-1) Antibody	Biolegend	Cat# 329935; RRID:AB_2563593
PE Mouse Anti-Mouse CD366 (TIM-3)	Biolegend	Cat# 345006; RRID:AB_2116576
Brilliant Violet 421™ anti-human CD223 (LAG-3) [11C3C65]	Biolegend	Cat# 369314; RRID:AB_2629797
Brilliant Violet 421™ anti-human CD62L [DREG-56]	Biolegend	Cat# 304828; RRID:AB_2562914
PE/Cy7 anti-human CD45RO [UCHL1]	Biolegend	Cat# 304229; RRID:AB_11203903
anti-human CD8A APC (REAfinity)	Miltenyi biotech	Cat# 130-110-679; RRID:AB_2659237
Anti-Human TNF alpha PE	eBioscience	Cat# 12-7349-82; RRID:AB_466208
Anti-Human CD3 Functional Grade Purified	eBioscience	Cat# 16-0037-85; RRID:AB_468855
Anti-Human LCK (3A5)	Santa Cruz Biotechnology	Cat# sc-433; RRID:AB_627880
goat anti-mouse IgG (H + L) secondary antibody Alexa Fluor 647	Thermo Fisher Scientific	Cat# A-21235; RRID:AB_2535804
IRDye 800CW Goat anti-Mouse IgG2b	LI-COR	Cat# 926–32352; RRID:AB_2782999
IRDye 680LT Goat anti-Rabbit	LI-COR	Cat# 926-68021; RRID:AB_10706309
HLA-A2-L2 TCR-like antibody	Paul A. MacAry lab[13]	N/A
Bacterial and virus strains		
NEB Stable Competent E.coli (High Efficiency)	New England Biolabs (NEB)	Cat# C3040H

(*Continued on next page*)

Continued

REAGENT or RESOURCE	SOURCE	IDENTIFIER
Biological samples		
human peripheral blood mononuclear cells (PBMCs)	Healthy donors	N/A
Chemicals, peptides, and recombinant proteins		
SFK inhibitor PP2	Sigma-Aldrich	Cat# P0042
Lectin from *Phaseolus vulgaris* (red kidney bean)	Sigma-Aldrich	Cat# L9017
polyethylenimine (PEI)	Sigma-Aldrich	Cat# 408727
NP-40 Alternative	Sigma-Aldrich	Cat# 492016
LCK inhibitor A770041	MedChemExpress	Cat# HY-11011
FYN inhibitor SU6656	SelleckChem	Cat# S7774
Indo-1, AM	Thermo Fisher Scientific	Cat# I1223
CellTrace™ Violet	Thermo Fisher Scientific	Cat# C34557
Dynabeads™ human T-activator CD3/CD28	Thermo Fisher Scientific	Cat# 11132D
GAG (SLYNTVATL) peptide	GenScript	N/A
LMP2A426-434 (CLGGLLTMV) peptide	GenScript	N/A
D-Luciferin	PerkinElmer	Cat# 122799
Biotarget medium	Biological Industry	Cat# 05-080-1A
Human platelet lysate (Ultra-GRO™-Advanced)	AventaCell	Cat# HPCFDCRL50
Human IL-2	R&D System	Cat# 202-IL-050
Human IL-7	R&D System	Cat# 207-IL-025
Human IL-15	R&D System	Cat# 247-ILB-025
LIVE/DEAD® Fixable Near-IR Dead Cell Stain Kit	Life Technologies	Cat# L34976
In-Fusion HD cloning kit	Clontech	Cat# 639648
Q5 mutagenesis Kit	New England Biolabs (NEB)	Cat# E0554S
Cas9-NLS protein	UC Berkeley-Qb3 lab	N/A
Protein Transport Inhibitor (Containing Brefeldin A)	BD	Cat# 555029
Protein G Dynabeads	Invitrogen	Cat# 10003D
Critical commercial assays		
IL-2 ELISA assay	Invitrogen	Cat# 88-7025-88
CytoTox 96® Non-Radioactive Cytotoxicity Assay	Promega	Cat# G1780
96-well RTCA E-plates	Agilent	Cat# 300601010
Experimental models: Cell lines		
Jurkat 76	Mirjam Heemskerk[47]	N/A
Raji	ATCC	Cat# CCL-86
Nalm-6	ATCC	Cat# CRL-3273
Daudi	ATCC	Cat# CCL-213
MCF-7	ATCC	Cat# HTB-22
SKBR3	ATCC	Cat# HTB-30
Jurkat cam1.6	ATCC	Cat# CRL-2063
Lenti-X	Takara Bio	Cat# 632180
Nalm-6-Luc	This manuscript	N/A

(*Continued on next page*)

Continued		
REAGENT or RESOURCE	SOURCE	IDENTIFIER
MCF-7-HER2	This manuscript	N/A
Experimental models: Organisms/strains		
NOD.Cg-Prkdc^{scid}IL2Rg^{tm1wjl}/SzJInv (NSG)	InVivos	Strain code: 005557
Oligonucleotides		
gRNA sequence for Cas9-KO	See Table S1	N/A
shLCK sequence: CTGCAAGACAACCTGGTTATC	Methi et al.[48]	PMID: 16301647
shNTC sequence: CCTAAGGTTAAGTCGCCCTCG	Sarbassov et al.[49]	PMID: 15718470
Recombinant DNA		
Anti-CD19 scFv (FMC63)	Laurence Cooper lab[50]	N/A
Anti-HER2 scFv (4D5-5)	Richard Morgan lab[51]	N/A
LMP2A specific TCR-like scFv	Paul A. MacAry lab[13]	N/A
CD28CAR	This manuscript	N/A
CD137CAR	This manuscript	N/A
pLV-shRNA-CAR	This manuscript	N/A
pLV	Vectorbuilder	N/A
pRP[Exp]-CMV > gag:pol:RRE	Vectorbuilder	VB160226-10009
pRP[Exp]-RSV > Rev	Vectorbuilder	VB160226-10011
pRP[Exp]-CMV > VSVG	Vectorbuilder	VB160226-10010
pcDNA3-Clover	Addgene	Cat# 40259
Software and algorithms		
FlowJo 10.0	FlowJo, LLC	https://www.flowjo.com/
GraphPad Prism version 7.0	GraphPad software	https://www.graphpad.com
RTCA 2.0	Agilent	https://www.agilent.com
ClustVis	University of Tartu	https://biit.cs.ut.ee/clustvis/
GSEA	Broad Institute	https://www.gsea-msigdb.org/gsea/index.jsp
GO	GO Consortium	http://geneontology.org/
The Human Protein Atlas	The Human Protein Atlas	https://www.proteinatlas.org/
DICE	La Jolla Institute for Immunology	https://dice-database.org/
String webtool	String Consortium	https://string-db.org/
DAVID Bioinformatics Resource	Laboratory of Human Retrovirology and Immunoinformatics	https://david.ncifcrf.gov/summary.jsp

RESOURCE AVAILABILITY

Lead contact

Further information and requests for resources and reagents should be directed to and will be fulfilled by the lead contact, Nicholas R.J. Gascoigne (micnrjg@nus.edu.sg).

Materials availability

Reagents generated in this study will be made available on request, but we may require a payment and/or a completed Materials Transfer Agreement based on NUS's legal requirement if there is potential for commercial application.

Data and code availability

All data needed to evaluate the conclusions in the paper are present in the paper or the supplemental information. This paper does not report original code. Any additional information required to re-analyze the data reported in this work paper is available from the lead contact upon request.

EXPERIMENTAL MODEL AND SUBJECT DETAILS

Cell lines and cell culture

Endogenous TCR and co-receptor-deficient Jurkat76 was a kind gift from Prof Mirjam Heemskerk[47] (Leiden Univ, NL). Other cell lines (Raji, Nalm-6, Daudi, MCF-7, SKBR3 including LCK-deficient Jurkat cam1.6) were from the American Type Culture Collection (ATCC). No commonly misidentified cell lines were used (ICLAC database). Jurkat lines were maintained in RPMI-1640 media (Hyclone) supplemented with 10% fetal bovine serum (Hyclone), 2 mM L-glutamine (Gibco) and MEM non-essential amino acid (Gibco) (cRPMI) in humidified 5% CO_2 incubator at 37°C. Human embryonic kidney epithelial cells (HEK293) were cultured in DMEM (Hyclone) supplemented with 10% fetal bovine serum (Hyclone), 2 mM L-glutamine (Gibco) and MEM non-essential amino acid (Gibco). Tetracycline-Regulated Expression (T-REx) CHO cell line was purchased from Invitrogen and used for the generation of artificial APC. The CHO cells were cultured in Ham's F-12 (Gibco) medium with 10% fetal bovine serum (Hyclone), 2 mM L-glutamine (Gibco) and MEM non-essential amino acid (Gibco). Transfections of Single-chain trimer MHC constructs into CHO were performed using the polyethylenimine (PEI) method. After transfection, cells were drug-selected (1.0 mg/mL G418, Hyclone), then single cell sorted. The pMHC complex expression was checked regularly by flow cytometry, and cell lines used were checked routinely to detect mycoplasma contamination.

Primary CD8$^+$ T cell activation and culture

Naive CD8$^+$ T-cells were isolated isolated from blood using RosetteSep human CD8$^+$ T cell enrichment cocktail (Stemcell) and Ficoll (GE Healthcare Life Sciences) gradient centrifugation. Naive CD8$^+$ T-cells were stimulated by anti-CD3$^+$CD28 Dynabeads (ThermoFisher) in Biotarget medium (Biological Industry) supplemented with 4% human platelet lysate (Ultra-GRO-Advanced, AventaCell) with 100U/mL IL-2 (R&D System) for 48hrs. Activated CD8$^+$ T-cells were maintained in medium containing 100 U/mL IL-2, 10 ng/mL IL15 and 10 ng/mL IL7 (R&D System). T-cells were restimulated every 14-20 days by feeder cells, which were freshly isolated peripheral blood mononuclear cells (PBMC) and irradiated at 30 Gy. PBMC and T-cells were resuspended at a ratio of 2:1 in the medium with concentrations of 100U/mL IL-2, 10 ng/mL IL7, 10 ng/mL IL15 and 1.5 μg/mL of Lectin from *Phaseolus vulgaris* (Sigma-Aldrich). Blood collection protocol was approved by NUS IRB. Informed consent was obtained from all donors.

In vivo animal model

NOD.Cg-Prkdc^{scid}IL2Rg^{tm1wjl}/SzJlnv (NSG) female mice, 6-8 weeks old, (InVivos) were used for in a standard leukemia model using Nalm-6 cells, which has been transduced with luciferase, and a solid tumor model using MCF7-HER2 cells. CAR-T-cells were sorted by FACSFusion sorter and restimulated by feeder cells at day −3. Cancer cells were administered intravenously (i.v.) via tail (Nalm-6) or subcutaneously (MCF7- HER2). Both cell lines produced even tumor burdens in our experiments, and no mice were excluded before treatment. Expanded CAR-T-cells were administered i.v. at day 4 after cancer cell injection or at day 5 after solid tumor initial growth. The mice were euthanized when paralysis was observed or tumor size exceeded 2000 mm^3. For *ex vivo* CAR-T-cell phenotyping, bone marrow and spleen cells were extracted and analyzed by FACS. Animal Protocols were approved by NUS IACUC.

METHOD DETAILS

Constructs and sequences

CARs with CD28 and CD137 costimulatory sequences were synthesized and cloned into lentiviral vector pLV. This and associated packaging plasmids, bearing Gag/Pol, Rev, and VSV-G respectively, were supplied by Vectorbuilder. Human *HER2* genes were cloned from a human cDNA library in-house. The scFv constructs for TCR-like antibodies[13] were produced in P.A.M.'s lab, and FMC63 scFv and 4D5 scFv were used for anti-CD19CAR and anti-HER2CAR, respectively.[50,51] TCR specific for HLA-A*02:01 with peptide LMP2A$_{426-434}$ (from EBV) was a generous gift from Hans Stauss (University College London). Single-chain trimer GAG-HLA-A2 was a gift from Keith Gould (Imperial College London). Peptide mutagenesis: GAG (SLYNTVATL) to LMP2A$_{426-434}$ (CLGGLLTMV) (L2); CD28 Y170F, P187,190A, and other mutations were made with Q5 mutagenesis Kit (New England Biolabs). Molecular cloning work used In-Fusion HD cloning kit (Clontech), and single-chain trimer MHC constructs were cloned into pcDNA3-Clover (Addgene plasmid #40259) to generate artificial antigen presenting CHO cells.[52–54] shRNA-CAR constructs were based on pLV-CAR vector described above, in which a cassette of the human U6 and shRNA sequence were added. shLCK sequence[48]:5′-CTGCAAGACAACCTGGTTATC-3′ shNTC sequence[49]: 5′-CCTAAGGTTAAGTCGCCCTCG-3′.

Lentivirus production and transduction

6.5 × 10^5 HEK293-Lenti-X cells/well were seeded onto 6 well plates one day before transfection and incubated at 37°C with 5% CO_2. The cells were transfected with packaging plasmids and lentiviral vector using polyethylenimine (PEI), and the medium replaced after 12h. Viral supernatant was harvested twice in the following 2days. The collected viral supernatant was titred, filtered through 0.45μm membrane (Millipore) and concentrated by ultracentrifugation filter (100kDa, Amicon). For lentivirus transductions, polybrene and HEPES were added at 8-10 μg/mL and 10mM, respectively, with Jurkat or CD8$^+$ T-cells after 48h initial activation by anti-CD3$^+$CD28 Dynabeads (ThermoFisher) at 10^6/mL, followed by spinoculation at 2,500 rpm for 2 hrs at 32°C. For CHO cell transduction, viral solution was directly added without spinoculation for 24h. Cells and viral solutions were separated after transduction.

CRISPR-Cas9 knock-out and knock-in genetic editing

Cas9 lentivector was obtained from Addgene (#52961).[55] The gRNA sequences for FYN and LCK were retrieved from http://chopchop.cbu.uib.no/and are shown in the Table S1. Cas9 sequence was linked with mTagBFP by P2A cleavable linker. The Cas9 lentivector was used to make lentivirus for transduction of Jurkat. Single cells were sorted by mTagBFP and western blotting was used to screen LCK or FYN KO Jurkat clones. In primary $CD8^+$ T cells, *LCK* targeted homologous directed repair (HDR) was performed as previously described.[56] The *LCK* gRNA2, GCCGGGAAAAGTGATTCGAG, was selected and chemically modified. Full sgRNA sequence was, 5′-G*C*C*GGGAAAAGUGAUUCGAGGUUUUAGAGCUAGAAAUAGCAAGUUAAAA UAAGGCUAGUCCGUUAUCAACUUGAAAAAG UGGCACCGAGUCGGUGCU*U*U*U-3'. Asterisk (*) represents 2′-*O*-methyl 3′ phosphorothioate. The Cas9-NLS protein (New England Biology) was incubated with sgRNA at a molecular ratio of 1:2 at 37°C for 30min to form ribonucleoprotein (RNP) complexes. The dsDNA donor was designed so that 1kb of the homologous arm was flanking the CAR construct on each side. 120pmol of RNP and 2μg of dsDNA were electroporated into 10^6 activated primary $CD8^+$ T-cells by Amaxa P3 Primary Cell Kit (V4XP-3024) and Amaxa 4D electroporation system (Lonza) via program EH115. The CAR + population was stained by anti-Myc tag conjugates (Cell Signaling Technology) and later sorted by FACSFusion sorter (BD) in flow cytometry core facility team of The Life Sciences Institute (LSI), NUS.

Calcium flux assay

The calcium flux assay was performed as previously described.[57] In brief, cells were suspended at 10^7/mL in PBS (PBS) and loaded with 2 μM Indo-1 AM for 30 min at 37°C, followed by washing twice with cRPMI. Cells were pre-warmed to 37°C for 10min before analysis and kept at 37°C during analysis. For cell stimulation, an HLA-A2-L2 monomer was pre-refolded, biotinylated[58] and cross-linked with streptavidin Alexa 647 (ThermoFisher) to form tetramer, that was used to stimulate cells. Mean fluorescence ratio of Indo-1^{high}/Indo-1^{low} was calculated using FlowJo kinetics program.

T cell stimulation and cytokine secretion assay

This was performed largely as described.[53,54] Artificial antigen presenting CHO cells (APC-CHO) were seeded onto a 96 well flat plate at 2–3x10^4/well one day before use. Each CAR-T-cell or TCR-T-cell sample was counted and 2 × 10^5 cells/well was added into APC-CHO pre-seeded plate for 18h. After incubation, supernatant was collected for IL-2 ELISA assay (Invitrogen). T cell pellets were resuspended for immunophenotyping or for another round of stimulation. For primary CAR-T-cell cytokine secretion, target cells (at 1:1 ratio) or precoated anti-CD3 antibody (5 μg/mL) were used to activate CAR signaling or endogenous TCR signaling, respectively. CAR-T-cells were stimulated together with Brefeldin A in one well of a 96 well plate for 6h. After stimulation, cells were collected and stained with anti-CD8 for T cell gating and anti-Myc to measure CAR expression. T-cells were then further permeabilized and stained with anti-TNF and IFNγ before FACS analysis. For proliferation experiments, CAR-T-cells labeled with CellTrace Violet and Nalm-6 cells were mixed at a ratio of 1:1 at 5 × 10^4 cells/well in 96 well plates. Cells were collected after 5 days and analyzed by FACS.

Cytotoxicity assay

Target cells were seeded at 4 × 10^4/well in U-bottom 96 well plates, followed by adding 4 × 10^3 to 4 × 10^5 CAR-T-cells at effector to target (E:T) ratio 0.1:1 to 10:1. Cells were cocultured for 18 h at 37°C, 5% CO_2. The supernatant was then collected, and the CytoTox 96 Non-Radioactive Cytotoxicity Assay (Promega) was used. Cytotoxicity (%) was calculated by formula ($LDH^{release}$-negative)/($LDH^{maxrelease}$-negative). The cell pellet was suspended and stained with antibody conjugates to do immunophenotyping. For real-time killing experiments, xCelligence (Agilent) was used. 2 × 10^4 CD19-transduced CHO cells (CHO-CD19) were pre-seeded in 96-well RTCA E-plates and incubated for 24h. CAR-T-cells were added at designated ratio. Cell growth was monitored for additional 36h.

Western blotting and immunoprecipitation (IP)

10^6 cells/sample were lysed in NP-40 lysis buffer. Cell debris was pelleted, supernatant collected and heated with reducing protein loading buffer (Nacalai-Tesque). To detect phosphorylation after stimulation, 10^5 APC-CHO cells were seeded per well in a 24-well plate one day before stimulation. 10^6 CAR-T or TCR-T-cells were added into each well and cocultured for the designated duration. Cells were collected and prepared as above. To detect FYN association with CAR, 10^7 CAR-Jcam cells and 2 × 10^6 CHO-L2 cells were mixed for 5min in 1mL cRPMI. Stimulation was stopped by adding 10mL pre-cooled PBS. Cells were collected and lysed in 200μL NP-40 lysis buffer. Lysate was incubated overnight with protein G Dynabeads (Invitrogen, 10003D) with anti-Myc. IP samples were washed in lysis buffer and heated with reducing protein loading buffer. All samples were loaded in a 4-12% Bis-Tris gradient gel (NuPAGE, Invitrogen) and transferred to a PVDF membrane (Immobilon-FL Transfer Membrane, Millipore). The membrane was blocked using blocking buffer (Odyssey, LI-COR). The membrane was probed with different primary antibodies, followed after washing by secondary antibodies: IRDye 800CW Goat anti-Mouse IgG2b (Cat# 926–32,352, LI-COR) and IRDye 680LT Goat anti-Rabbit (Cat#926-68021). Visualization and quantification of the blot was by the LI-COR Odyssey infrared imaging system.

Flow cytometry and cell sorting

Flow cytometry experiments were conducted on BD LSR Fortessa X-20 (Becton Dickinson). Cell sorting was conducted on either Mo-Flo XDP (Beckman Coulter, Inc.) or SY3200 (Sony Biotechnology Inc.) by Flow Cytometry Laboratory, Immunology Program, National University of Singapore. Data analysis was performed on FlowJo.

Signal pathway analysis

The ''T-cell receptor pathway'', ''T cell signaling'', ''T cell activation'', ''T cell stimulation'', ''T cell costimulation'', and ''T cell inhibitory signaling'' were queried in GSEA (https://www.gsea-msigdb.org/gsea/index.jsp), GO (http://geneontology.org/), and NCBI to create a total TCR signaling-related molecules pool. The molecules in the pool were later screened by their expression in Naive or activated $CD8^+$ T-cells via The Human Protein Atlas (https://www.proteinatlas.org/) and Database of Immune Cell Expression (DICE) (https://dice-database.org/), where the proteins with low or no expression in CD8 T cells were filtered out. These filtered signaling molecule pools were then the ''TCR signaling molecules pool''. Signaling molecules within the ''TCR signaling molecules pool'' that interact to FYN or LCK and their respective link score were acquired via String webtool (https://string-db.org/). Signal pathway identification was done by analyzing the FYN or LCK group molecules (described in the main text) in KEGG pathway database via DAVID Bioinformatics Resource (https://david.ncifcrf.gov/summary.jsp).

Statistical information and data analysis

Two-tailed Student's *t* test or two-way ANOVA analysis was performed for column data or curve data respectively by using GraphPad Prism 7. The data meet the assumptions of the tests. Variance is similar between the compared groups. For principal component analysis (PCA), *in vivo* performance factors were consolidated, and the data analyzed by ClustVis (https://biit.cs.ut.ee/clustvis/), obtaining converted PCA values for each factor acquired.

Cell Reports Medicine, Volume *4*

Supplemental information

CD28-CAR-T cell activation through FYN kinase signaling rather than LCK enhances therapeutic performance

Ling Wu, Joanna Brzostek, Previtha Dawn Sakthi Vale, Qianru Wei, Clara K.T. Koh, June Xu Hui Ong, Liang-zhe Wu, Jia Chi Tan, Yen Leong Chua, Jiawei Yap, Yuan Song, Vivian Jia Yi Tan, Triscilla Y.Y. Tan, Junyun Lai, Paul A. MacAry, and Nicholas R.J. Gascoigne

Table

CRISPR-Cas9 guide RNA (gRNA) sequences for LCK and FYN knock out. Related to STAR method.

gRNA	Sequence
LCK gRNA1	GACCCACTGGTTACCTACGA
LCK gRNA2	GCCGGGAAAAGTGATTCGAG
FYN gRNA1	AGAGTTCACACCTCCAAAGA
FYN gRNA2	ACGGGGACCTTGCGTACGAG
FYN gRNA3	TTGTCCTTTGGAAACCCAAG
FYN gRNA4	GTCCCCCGAATCATTCCTTG
FYN gRNA5	TGGATACTACATTACCACCC

gRNA pool for LCK and FYN knock out. Each of gRNA was selected from http://chopchop.cbu.uib.no/. After screening, LCK gRNA2 and FYN gRNA3 were chosen for LCK and FYN knock out respectively.

Figures

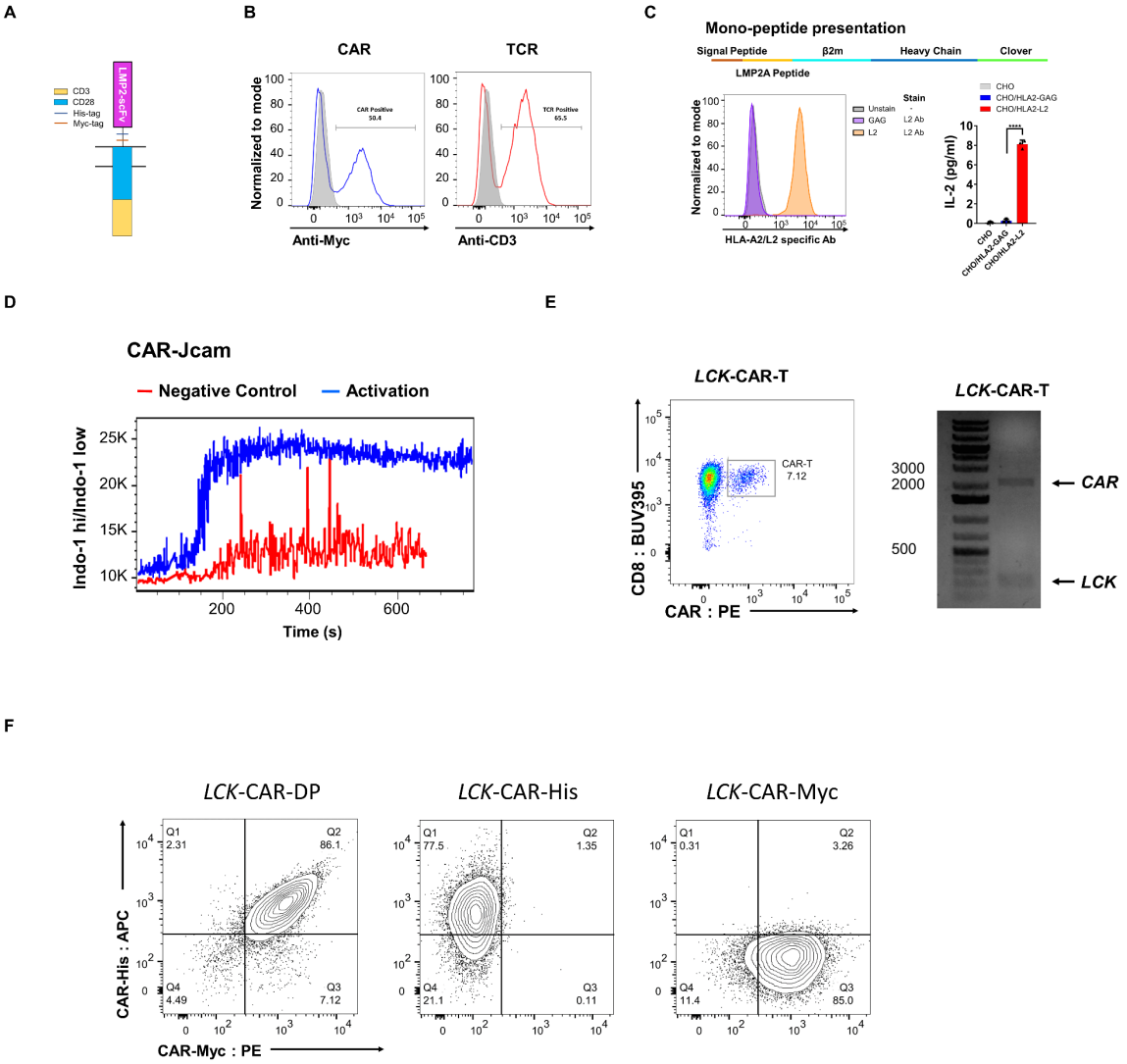

Figure S1. CAR signaling does not require LCK. Related to Figure 1. (**A**) Schematic diagram of CAR construct. Myc-tag was used for the detection of CAR expression. (**B**) Expression of LMP2A peptide (L2)-specific CAR or TCR after lentiviral transduction of Jurkat76. CAR was stained using anti-Myc, TCR with anti-CD3 Abs. (**C**) Schematic diagram of the scHLA construct with linked peptide ("mono-peptide system": upper). Lower left: staining with L2-specific TCR-like Ab on CHO-L2 or CHO-GAG. Lower right: responsiveness of L2-specific CAR-T to CHO-L2 versus CHO-GAG. Mean ±SD of technical triplicates, from 3 experiments. (**D**) Ca^{2+} flux of CAR-Jcam cells. Negative control was PBS, activation by adding specific pMHC tetramer. (**E**) *LCK* locus-

18 targeted CRISPR-Cas9 editing. Left panel shows the percentage of $CD8^+$ CAR^+ CAR-T cells after editing. Right
19 panel is the genotyping of the targeted site in the *LCK* gene. Forward primer: 5'-
20 AGGGAGAGGTGGTGAAACATTA-3', reverse primer: 5'- GAATGGAGTAGGGCATTGAAAG-3'. (**F**)
21 CAR-His and CAR-Myc expression after HDR and cell sort.

22

23

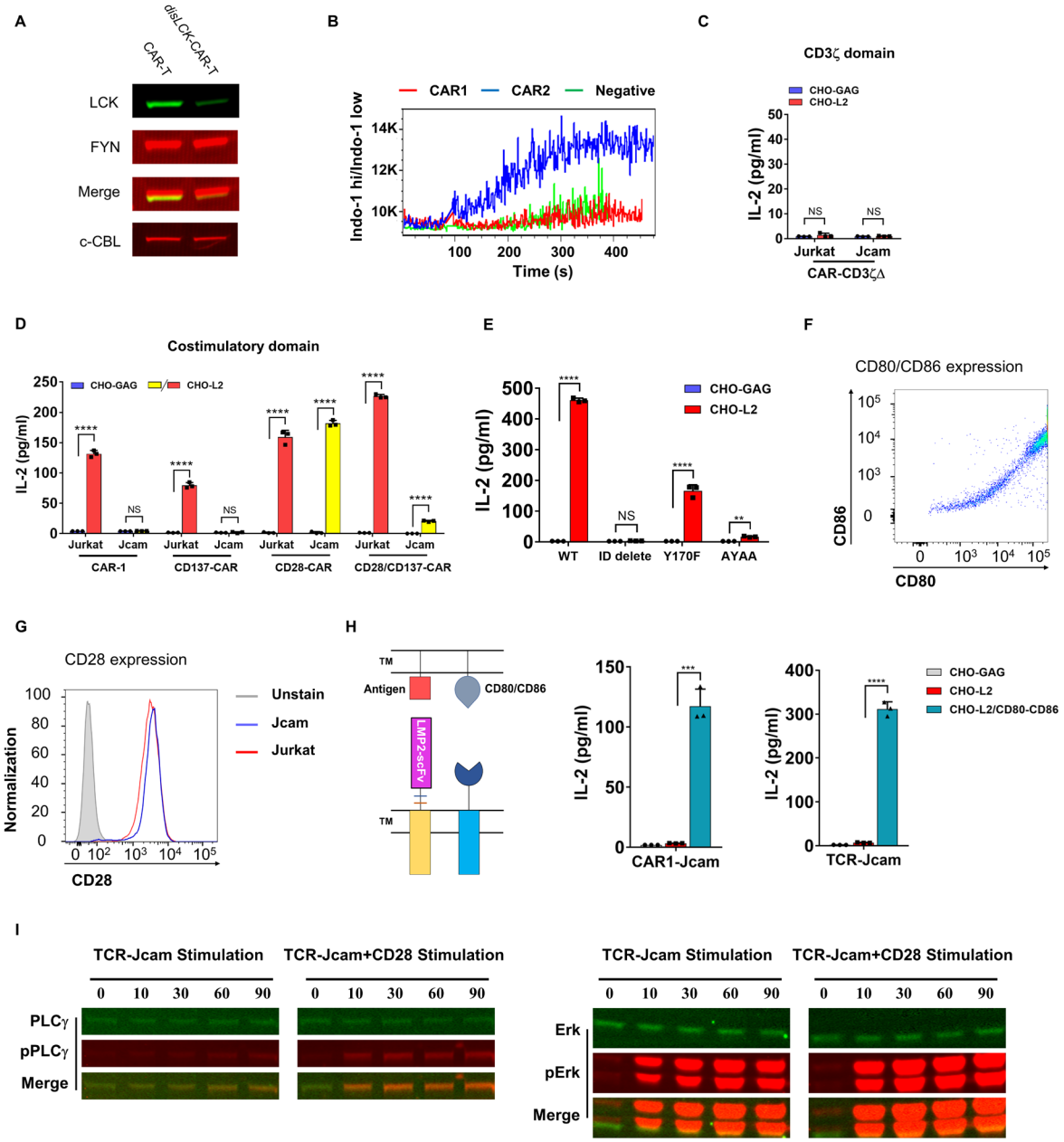

Figure S2. LCK-independent CAR signaling requires CD28 as costimulatory domain. Related to Figure 2.

(**A**) LCK protein expression of sorted *disLCK*-CAR-T cells in comparison with conventional CAR-T. (**B**) Calcium flux of CAR2-Jcam or CAR1-Jcam after specific HLA-A2-L2 tetramer was added into the medium. The second generation CAR with CD28 costimulatory domain in Jcam1.6 cell is labeled as CAR2-Jcam, and the first generation of CAR in Jcam1.6 cell is labeled as CAR1-Jcam. (**C**) IL-2 production of CAR constructs without CD3ζ signaling domain in Jurkat or Jcam cells. (**D**) IL-2 production of CAR constructs with different intracellular domains in Jurkat or Jcam cells. (**E**) IL-2 production of Jcam cells expressing different CD28-CAR mutants. (**F**)

Co-expression of CD80 and CD86 on CHO-L2 APC. The CD80 and CD86 were linked by P2A cleavable linker. CD80-P2A-CD86 construct was on one lentivirus vector. (**G**) Endogenous CD28 expression on Jurkat or Jcam1.6 cell lines. (**H**) Schematic of CD28 costimulation of CAR1 on JCam1.6 T cells and their responsiveness in Jcam1.6 to CHO-L2 expressing co-stimulators CD80 and CD86. (**I**) Phosphorylation of TCR signaling pathway with or without endogenous CD28 costimulation.

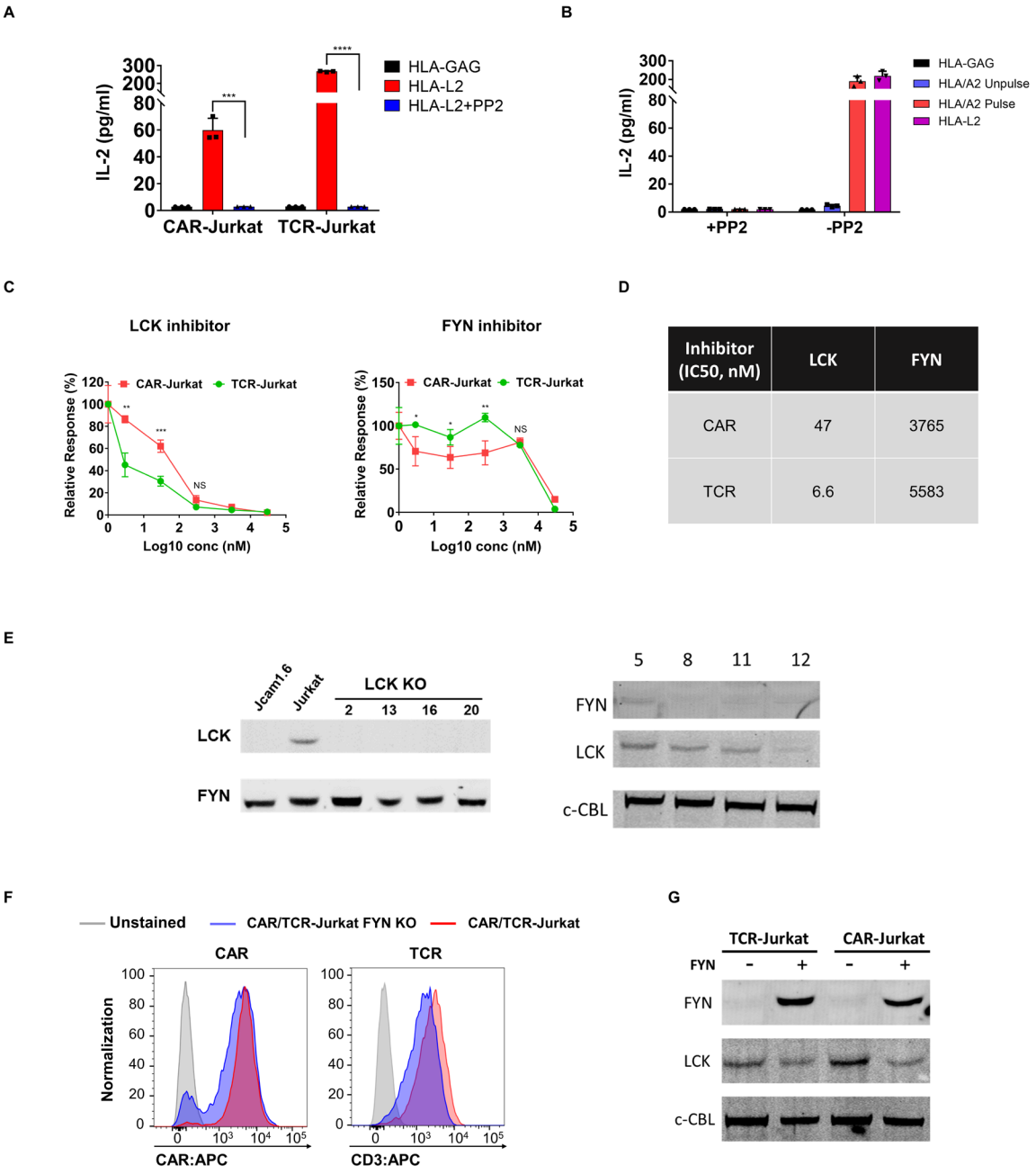

Figure S3. CD28-CAR relies on FYN to transduce downstream signaling. Related to Figure 3. (**A**) Responsiveness of CAR and TCR-Jurkat with SFK inhibitor PP2 (10μM). (**B**) IL-2 production of CAR-Jcam cell with or without SFK PP2. (**C**) Responsiveness of CAR and TCR-Jurkat in the presence of LCK or FYN inhibitors A770041 or SU6656, respectively. IL-2 production was normalized to that without inhibitors as the relative response (%) against log (inhibitor concentration). (**D**) IC50 of LCK- or FYN-specific inhibitors on CAR-Jurkat or TCR Jurkat cell. (**E**) LCK KO and FYN KO single clone selection. Clone 20 in LCK KO was selected as Jurkat LCK KO cell, and Clone 8 in FYN KO was selected as Jurkat FYN KO cell. (**F**) The CAR or TCR expression

47 detection on CAR-Jurkat FYN KO and CAR-Jurkat or on TCR-Jurkat FYN KO and TCR-Jurkat. CD3 was used
48 as an indicator of TCR expression. (**G**) FYN and LCK expression in CAR-Jurkat FYN KO and CAR-Jurkat or on
49 TCR-Jurkat FYN KO and TCR-Jurkat.

50

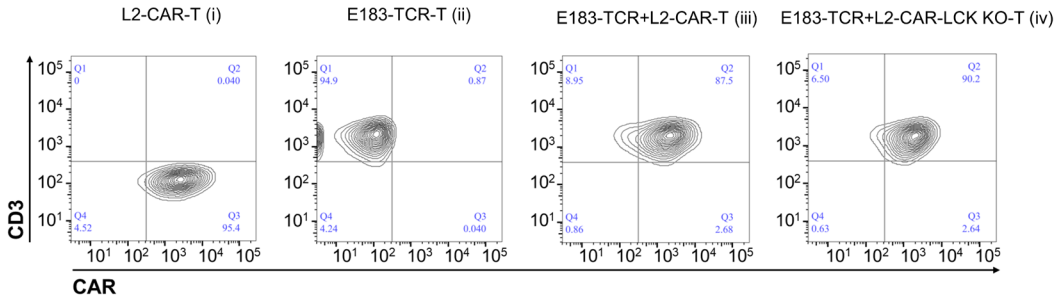

Figure S4. CAR or TCR expression on LCK-sufficient or deficient Jurkat after transduction and cell sort. Related to Figure 4. The TCR is specific for a peptide epitope from HBV antigen, E183. CAR was with the specificity as above, the peptide epitope (L2) from LMP2A protein.

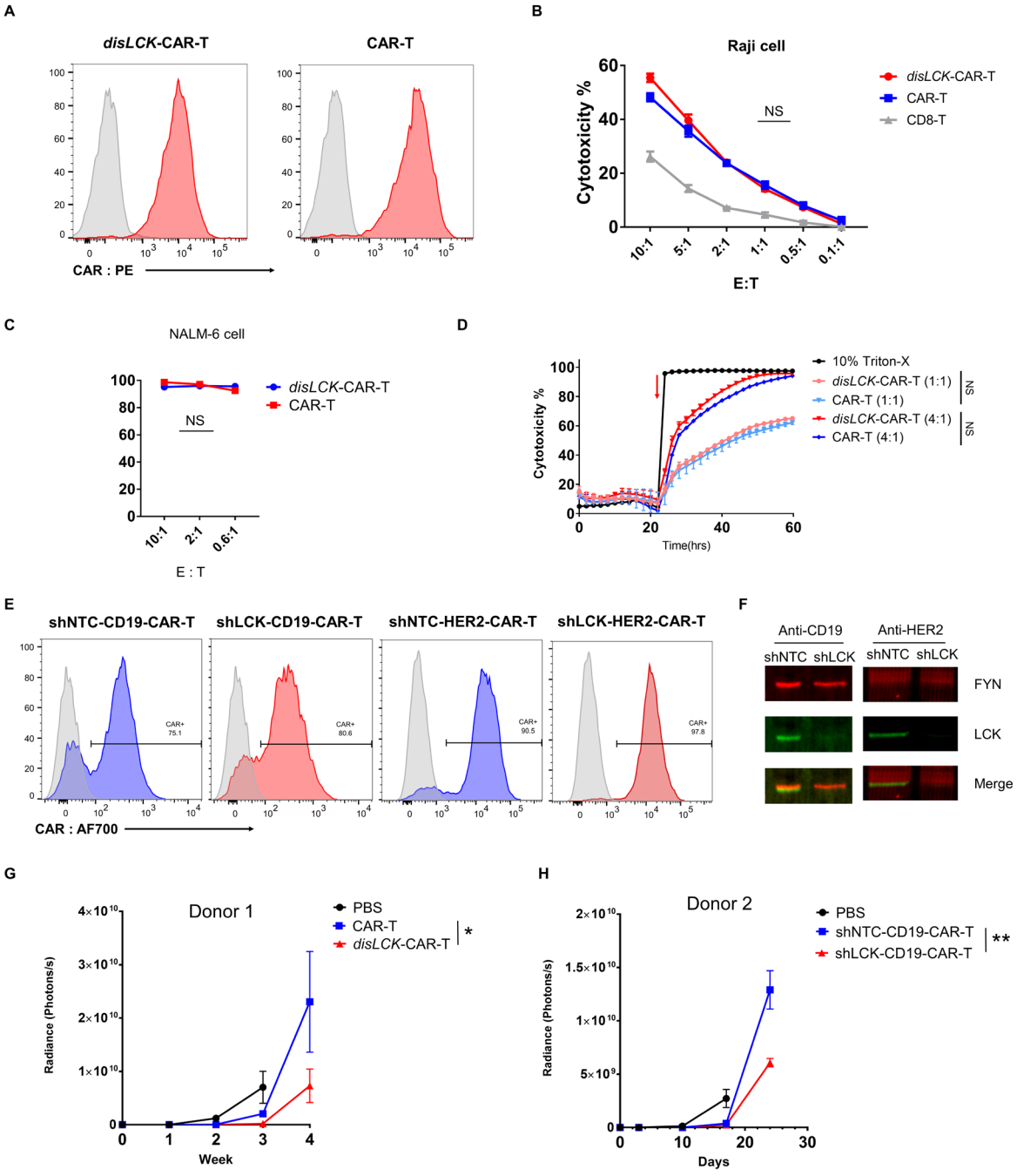

Figure S5. *In vitro and vivo* performance of disLCK-CAR-T cells. Related to Figure 5. (**A**) CAR expression of *disLCK*-CAR-T and conventional CAR-T after sorting and restimulation by feeder cells. Cytotoxicity of conventional CAR-T and *disLCK*-CAR-T to Daudi cells (**B**) and Nalm-6 cells (**C**). (**D**) Real time killing by two conventional CAR-T and *disLCK*-CAR-T cells to CD19-expressing CHO cells. The cytotoxicity was calculated by the formula: 1-cell index(sample)/cell index(media). (**E**) CAR expression of shRNA-CAR-T cells after sorting and restimulation by feeder cells. (**F**) LCK protein expression of sorted shRNA-CAR-T cells. (**G**, **H**) *In vivo*

luciferase signal from Nalm-6 cells at different time points. 2-way ANOVA was used to test the statistical significance.

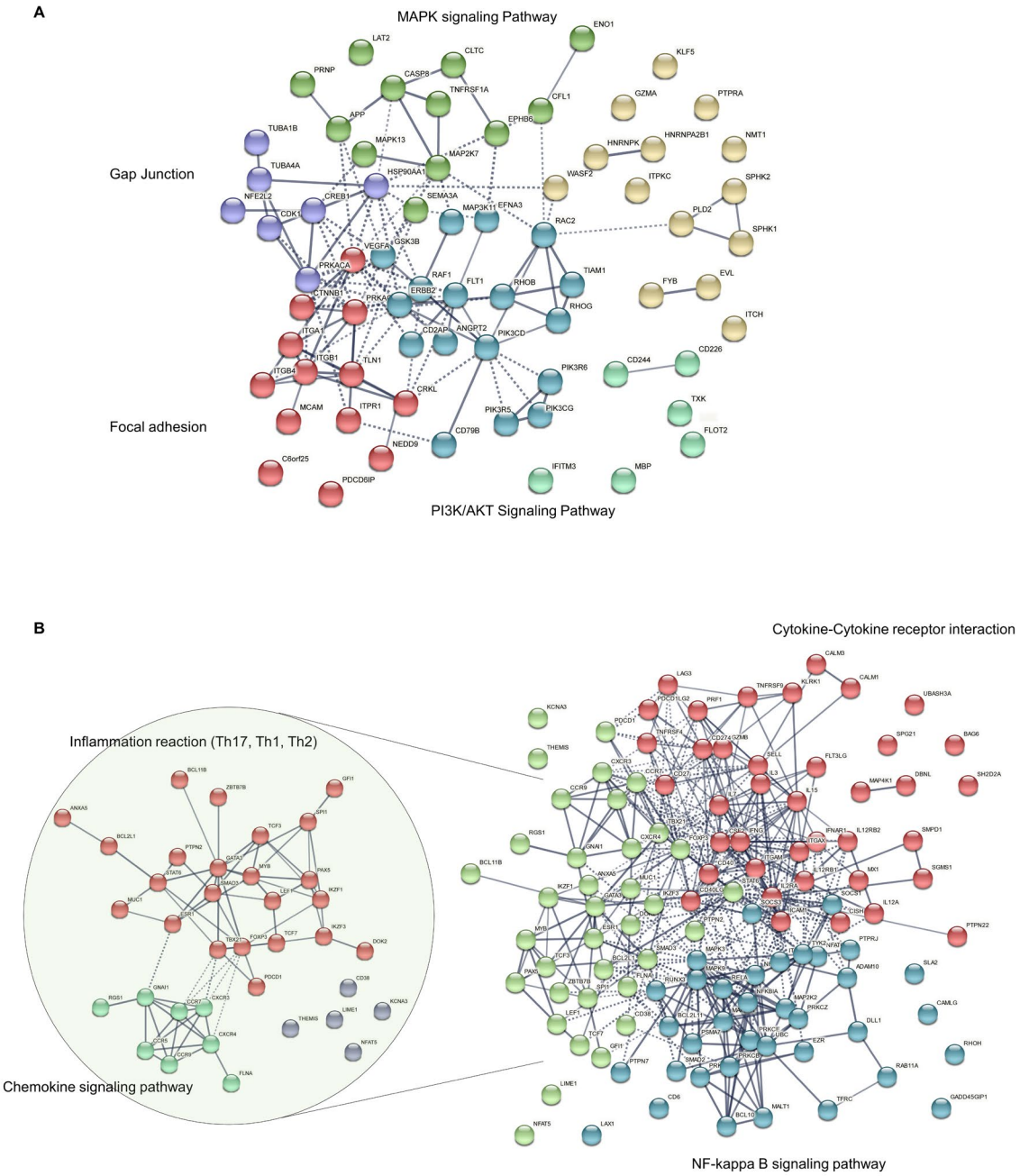

66

67 **Figure S6. Clustering of molecular interactions within FYN and LCK group. Related to Figure 6.** Cluster
68 of molecular interactions within FYN group (**A**) and LCK group (**B**). The cluster is identified by kmeans=6 (FYN
69 group) and =3 (LCK group). The analysis was done by String webtool analysis. The identification of signal
70 pathway was done by KEGG pathway database.

71

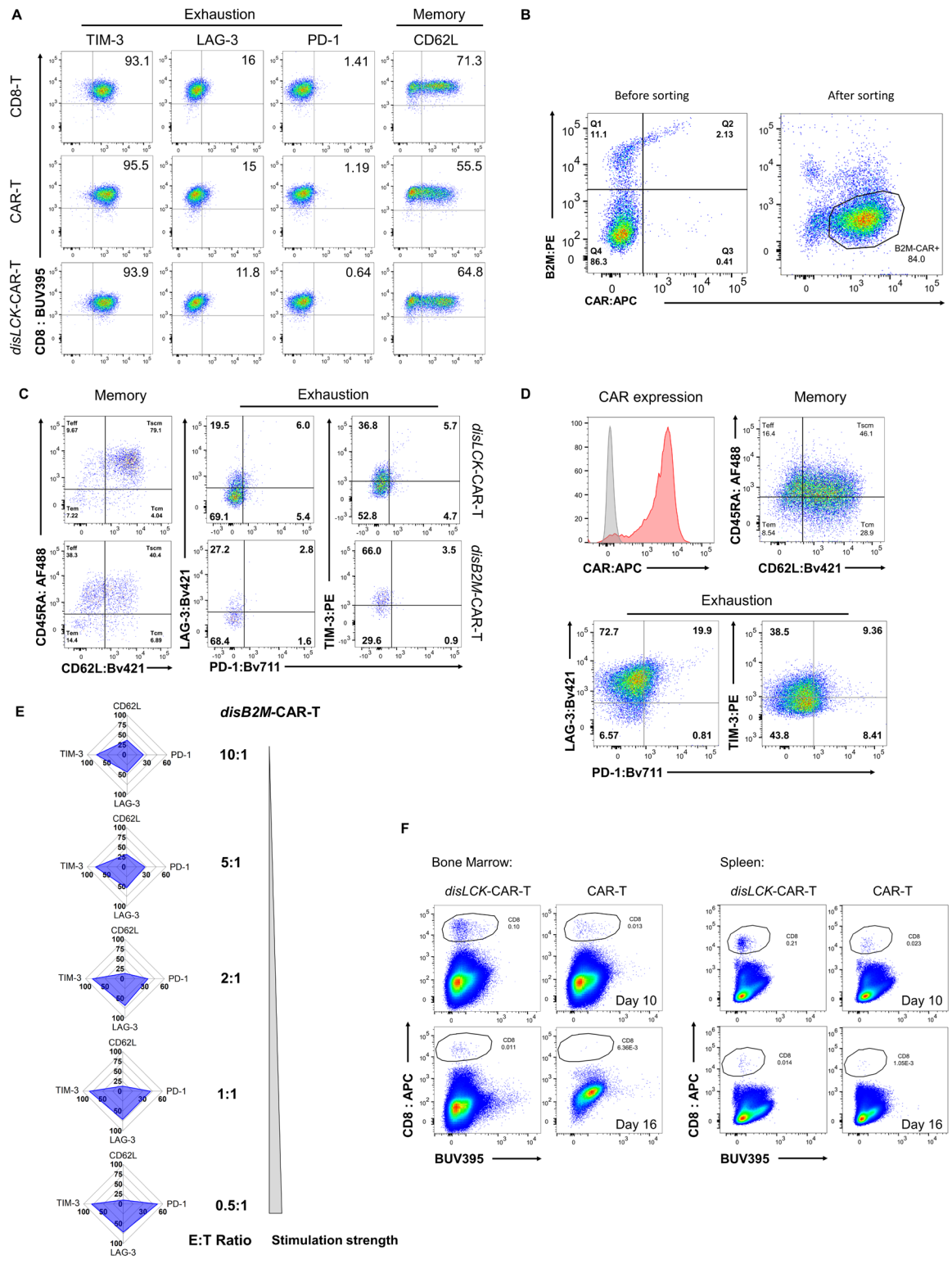

Figure S7. Independence from LCK makes CAR-T cells more specific, memory-like and less exhausted. Related to Figure 6 and Figure 7. (**A**) The memory and exhaustion state of *disLCK*-CAR-T and conventional CAR-T in quiescent state. The data is from another donors' T cells. (**B**) CAR and B2M expression after *B2M* locus-targeted HDR. *disB2M*-CAR-T cells were generated by using gRNA, GGCCGAGAUGUCUCGCUCCG,

through the same process as *disLCK*-CAR-T cells. (**C**) Comparison of the immunotyping of the *disB2M*-CAR-T and *disLCK*-CAR-T cells at resting state. The cells were gated before cell sort. (**D**) *disB2M*-CAR-T cells immunophenotype at day 5 after CAR-T cells sorting and restimulation by feeder cells. (**E**) Radar chart summary of exhaustion and memory marker expression in *disB2M*-CAR-T cells after encountering target cells at different E:T ratios. (**F**) Representative FACS graphs of CAR-T cells in bone marrow and spleen at day 10 and day 16.